AD

INCREASING ELECTROCHEMICAL MACHINING RATES

FINAL REPORT

by

N. H. COOK
S. P. LOUTREL
M. C. MESLINK

JANUARY 16, 1967

MASSACHUSETTS INSTITUTE OF TECHNOLOGY
CAMBRIDGE, MASSACHUSETTS.

DA-19-066-AMC-268(W)

U. S. ARMY MATERIALS RESEARCH AGENCY
WATERTOWN, MASSACHUSETTS 02172

124

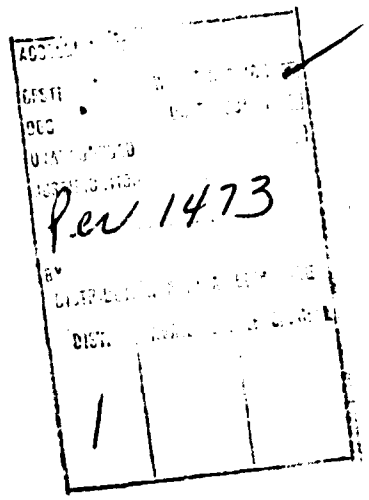

Mention of any trade names or manufacturers in this report shall not be construed as advertising nor as an official indorsement or approval of such products or companies by the United States Government.

The findings in this report are not to be construed as an official Department of the Army position, unless so designated by other authorized documents.

DISPOSITION INSTRUCTIONS

Destroy this report when it is no longer needed.
Do not return it to the originator.

INCREASING ELECTROCHEMICAL MACHINING RATES

FINAL REPORT

by

N. H. Cook

S. P. Loutrel

M. C. Meslink

January 16, 1967

Massachusetts Institute of Technology

Cambridge, Massachusetts

DA-19-066-AMC-268(W)

ABSTRACT

INCREASING ELECTROCHEMICAL MACHINING RATES

N. H. Cook, S. P. Loutrel and M. C. Meslink
Massachusetts Institute of Technology

Phenomena which may limit the rate of Electro-Chemical-Machining (ECM) are postulated, and indirectly studied by attempting their elimination. Of the mechanisms studied three appear most promising:

1. Elevated electrolyte pressure in the ECM zone reduces boiling, cavitation, and formation of hydrogen bubbles. As a result, drilling rates of 1.5 in/min have been attained at current densities up to 19,700 amps/in^2. This can be compared with a typical "maximum" rate of 1/4 in/min.

2. The use of fused salt electrolytes (such as NaOH) appears quite promising for difficult-to-ECM materials such as tungsten-carbide.

3. Pulsed DC current with short reverse spikes appears promising for materials such as tungsten-carbide which normally form relatively impervious reaction layers.

TABLE OF CONTENTS

	Page
Title Page	i
Abstract	ii
Table of Contents	iii
List of Illustrations and Photographs	iv
Nomenclature	vi
I. Introduction	1
II. Experimental Equipment	3
2-1 Mechanical System	3
2-2 Electrolyte Supply System	5
2-3 The Power Supply	6
2-4 Development of Tool and Insulation	14
III. Drilling Tests in the Pressure Chamber	18
3-1 Theory	18
3-2 1080 Steel (40 VDC)	22
3-3 1080 Steel (80 VDC)	30
3-4 Tungsten-Carbide	31
3-5 Inconel 600	33
3-6 Stellite J	34
3-7 Summary of Drilling Tests	35
IV. Molten Salt Electrolytes	36
V. Laser Tests	43
VI. Conclusions and Recommendations	46
VII. Acknowledgements	49
Appendix	
I. Fused Salt Data	50
II. Hole Drilling Data	58
III. The Laser	70
IV. Tool Data	72
V. Testing Procedure	73
VI. Illustrations	75
VII. Photographs and Detailed Drawings	96
Bibliography	112
Distribution List	114
DD Form 1473	117

LIST OF ILLUSTRATIONS AND PHOTOGRAPHS

		Page
2-1	Mechanical System (Atmospheric Pressure)	76
2-2	Pressure Chamber	77
2-3	ECM Fluid Feed System	78
2-4	Optimized Wave Shape	79
2-5	Block Diagram of ECM Power Supply	80
2-6	High Current Switch	81
2-7	High Current Components	82
2-8	Trigger Circuit	83
2-9	Revised Trigger Circuit	84
2-10	Electro Tool AA	85
2-11	Tool Types	86
3-1	Assumed Tool-Workpiece Geometry	87
3-2	Pressure Chamber Evaluation	88
3-3	Pressure Reduction - Gap Width	89
4-1	Fused Salt Apparatus	90
4-2	Weight Loss per Unit Depth vs Time	91
4-3	Weight Loss vs Current x Time	92
4-4	Current vs Voltage	93
4-5	Maximum Current Density Apparatus	93
5-1	Laser and ECM Cell	94
A3-1	Laser and Circuit Diagram	95
A7-1	Overall Milling Machine Setup	97
A7-2	Pressure Chamber	98

		Page
A7-3	Workpiece Mounted (Pressure Chamber Removed)	99
A7-4	Pressure Regulating Equipment	100
A7-5	Electrolyte Feed System	101
A7-6	Auxillary Drive Motor	102
A7-7	Power Supply	103
A7-8	D.C. Power Supplies	104
A7-9	Electrical Recording Equipment	105
A7-10	Tools and Workpieces	106
A7-11	Atmospheric Test Specimen	107
A7-12	Electro-Chemical Tool Holder	108
A7-13	Tool Lock-Nut	109
A7-14	Pressure Chamber Base	110
A7-15	Pressure Chamber Barrel	111

NOMENCLATURE

A	Amplitude
A	Atomic Weight (grams)
C	Capacitance
C_c	Coefficient of Cooling
D	Diameter
F	Flow Rate (in^3/min)
F_o	Faraday's Constant (96,500 amp-sec)
I	Current (amp
j	Current Density (amps/in^2)
M	Machining Rate (in^3/sec)
n	Unit vector normal to a streamline
P, p	Pressure (psi)
dp/dn	Rate of change of pressure normal to streamline
R	Resistance
r	Radius
T	Temperature
t	Time
V	Voltage
V_f	Fluid flow velocity (in/sec)
v	Machining Velocity (in/min)
dV/dt	Time rate of change of voltage

W	Weight
$\Delta W/\Delta T$	Time rate of weight removal
Z	Chemical Valence
γ, ρ	Density (lb/in^3)

INTRODUCTION

Electro-chemical-machining (ECM) has developed into a significant manufacturing process since World War II. It has been proven economically effective in drilling holes of various cross sections, die sinking, contouring, etc. Typical commercial ECM equipment operates in the vicinity of 15 VDC, at current densities ranging from 100-200 amps/in^2 in die sinking to perhaps 2000 amps/in^2 in hole drilling. The volume rate of metal removal is directly proportional to total current, and the rate of tool advance (feed rate) is therefore directly proportional to current density. At typical "state of the art" current densities, the maximum feed rate (machining steel) is about 1/4 in/min. When machining tungsten carbide, the rate is approximately zero!

There are various possible mechanisms which limit the ECM rate. Excluding machine limitations (current, speeds, etc.), the apparent limitations are:

1. Electrolyte boiling
2. Electrolyte cavitation
3. Hydrogen bubbles in the electrolyte
4. Anode or cathode films
    a. Polarized layers
    b. Reaction products
    c. Oxide layers
5. Electrode arcing

It is the purpose of this research to investigate a number of possible methods for removing the various ECM limitations. Our goals are twofold:

1. To increase the rates of ECM, and
2. To understand when the various limitations are operative.

The physical actions that we have used to alter the ECM process are:

1. High electrolyte velocity
2. High electrolyte pressure in cutting zone
3. High temperature (fused salt) electrolytes
4. Pulsed DC power
5. Elevated voltages
6. Incidence of Laser energy upon the surface being machined.

In order to study the process, we chose a simple drilling geometry for the majority of the tests. This permitted high current densities without requiring large total currents.

Chapter II

EXPERIMENTAL EQUIPMENT

2-1 MECHANICAL SYSTEM: (Fig. 2-1)

To obtain a very rigid feed system a horizontal milling machine is used with the tool holder mounted on the over-arms and the plexiglas tank and work holder mounted on the table. The vertical feeds of the milling machine are used to feed the tool and an auxillary motor drive is used to drive the milling machine at 1/6 of normal speed. This gives us the range of feeds required. The gross measurement of the position of the tool in the workpiece is made by a steel scale fixed to the carriage and read by an index line fixed to the over-arm assembly. For machining at atmospheric pressure without the pressure chamber, the work is clamped on the base piece in the plexiglas tank. The tank is covered with a plexiglas top to prevent splattering.

There is an exhaust line from the tank to a blower to draw out any hydrogen and oxygen gas that may be caused by electrolysis. Such gasses could conceivable cause an explosion ignited by sparks from the cutting zone.

Pressure Chamber; (Fig. 2-2)

For testing in a pressurized environment the workpiece and tool are placed in a stainless steel pressure chamber. The workpiece is mounted in bakelite which is clamped on top of the contact electrode.

The base zone of the workpiece is sealed with an o-ring seal to prevent entrance of electrolyte and subsequent machining of he electrode and base of the specimen. The specimen is held down by a steel washer with a delrin insulating washer under it.

The tool holder seals the top of the chamber and slides in the o-ring seals in the top of the chamber. The pressure chamber bolts to the base plate in the plexiglas tank and is aligned with the tool holder by adjusting the horizontal table feeds.

Electrical Connections to the Tool and Workpiece;

The tool holder and the stainless steel base piece in the plexiglas tank are insulated from their surroundings.

For D.C. Milling without the pressure chamber, the tool holder is grounded and is the negative terminal. The base piece is the "hot" positive terminal.

For D.C. Milling with the pressure chamber, the tool holder, basepiece, and thus the tank are all negative ground. The contact electrode is the "hot" positive terminal. In this way, the contact electrode is the only part of the chamber that is at the "sacrificial" potential.

For pulsed positive and negative current it is possible to entirely "float" all of these terminals though this should not be necessary. It is a very good safety precaution to be able to ground the tank, tool holder, and milling machine. Whether the terminals are all "floated" or some grounded, the pressure chamber, base piece, and the tool holder

must be electrically tied together.

A knife switch has been placed in the contact electrode power feed line to allow for making resistance measurements to check the bottom o-ring seal for leaks.

2-2 ELECTROLYTE SUPPLY SYSTEM: (Fig. 2-3)

The electrolyte is stored in a tank and fed to a low pressure centrifugal pump which pumps it through a filter to a high pressure pump. The high pressure pump is driven by compressed air and raises the fluid pressure to about 3000 psi. Pumping fluctuations are damped by the accumulator, a 2" I.D. cylinder with a piston backed by pressurized nitrogen to about 2000 psi. The fluid pressure then drives the piston about half way up the cylinder. The piston oscillates about this position to damp pumping transients.

From the accumulator the fluid is throttled through a valve into the tool holder and then into the tool. If the test is to be at atmospheric pressure the fluid passes through the tool and cutting zone and is caught in the plexiglas tank where it drains back through the drain line to the storage tank.

If the test is to be run in the pressure chamber the fluid passes through the tool and cutting zone into the pressure chamber. From the chamber it passes through the throttle valve and a pressure regulator and then into the drain line back to the tank. Either the throttle valve or a pressure regulator may be used to regulate chamber pressure.

Part of the flow through the centrifugal pump is returned directly to the tank thus maintaining a non-cavitating flow through the pump and continuously mixing the fluid in the tank.

There is a cooling or heating coil in the tank using hot or cold water to control the temperature of the electrolyte.

There is also a fresh water flushing system allowing us to isolate the storage tank and run fresh water through the entire system and down the drain thus flushing all electrolyte from the system. The filter is back flushed with fresh water.

Gages are placed to measure electrolyte supply pressure at the accumulator, accumulator nitrogen pressure, tool feed pressure, and chamber pressure. Flow rate can be measured by counting the stroking rate of the positive displacement pump.

Leakage from the high pressure pump seals is caught in a drip pan and run to the drain Leakage from the pressure regulator is channeled to the drip pan.

The entire supply system is constructed of stainless steel and plastic with the exceptions of the nickel plated steel accumulator, the painted steel tank, and the expendable cast iron centrifugal pump

2-3 THE POWER SUPPLY

One of the primary problems encountered in E.C.M. is the formation of passive films (oxides, sulfides, etc.) on the electrode surfaces. These films limit the total current and current density which in turn limits the rate at which material can be removed. In certain instances

high fluid velocities will overcome this film problem. With many materials, tungsten carbide being a prime example, these films build up so fast and heavily that the rate of material removal is essentially zero even under conditions of very high fluid velocity.

Since these films build up under direct current conditions, a periodic reversal of the current seems to be a possible solution to the problem. In other words, alternating current might eliminate the film problem. A simple laboratory experiment has shown this to be true. Alternating current is by no means the full solution, since the cathode (tool) is machined at the same rate as the anode (workpiece). From this evolved the idea of a variable frequency, variable positive and negative pulse width, and amplitude power supply. The idea being optimization in such a way that the negative pulse is just the right size to remove the film but not large enough to machine the cathode. This idea is illustrated in Figure 2-4. In Figure 2-4 we see a standard square wave and an optimized square wave. The proper ratio of t_1 to t_2 and A_1 to A_2 for maximum rate of removal should be determinate from experimentation.

Prior work conducted at M.I.T. indicated that we should consider frequencies in the range of 500 to 3000 cps. with a $t_1 : t_2$ ratio of 100 : 1 or greater. These frequencies are low from the point of view of a person working in the electronics field, but the task takes on a new light when we consider switching 100 amps or more at these frequencies.

In the laboratory we have available two portable rectifier units capable of delivering up to 120 amps at 0-120 V.D.C. The most direct means of obtaining the desired output seemed to be by running the outputs from both of these units into a variable frequency chopper, with one unit supplying the positive pulse, and the second supplying the negative. Numerous inquiries were made as to the possibility of obtaining such a unit as an "off the shelf" item, but it proved to be unavailable. Several electronic equipment manufacturers were contacted but this chopping device proved to be more than most were willing to handle. Finally two companies were found willing to consider the job. Their price quotations ranged from $6,000 to $10,000, with a minimum three month delivery time. From the point of view of the research work we were trying to accomplish the above quotations seemed like an unwarrented expenditure of time and money.

The following alternative possibilities were investigated:

1. Relays - Although a simple and direct approach, they proved unsatisfactory with an upper frequency limit of 5 cps.

2. Power amplifiers - We would not use the available power supplies Instead, we would use amplifiers and a wave generator. Audio amplifiers as used in high fidelity audio systems would not be suitable since they would not match the low load impedance of the E.C.M. process, and it is not possible to connect such amplifier outputs

in parallel to obtain the desired current capability. One electronics firm could supply a suitable amplifier, but at the prohibitive price of $9,00[illegible].

3. Mercury Switch - A somewhat unconventional method using a contact vibrating in a pool of Mercury was considered. A crude experiment was conducted in which a square wave at 300 cps was generated. However, such a set-up had far less than the current capability needed.

After considering all of the above and the high cost of having a finished piece of equipment manufactured, it seemed well worth the effort to try to design and build our own switching circuit similar to those proposed by the electronic equipment manufacturers.

The basic element of the high current, high frequency switching circuit is the silicon controlled rectifier (SCR). The SCR is a semiconductor that can be operated as a switch with a turn-on time in the range of microseconds. Unlike the vacuum tube or transistor both, of which are basically variable resistances and require a continuous "on" signal to remain conducting, the SCR can be turned on by the momentary application of a small control current to the gate. It remains conducting even after removal of the gate current. Furthermore, SCR's are available for handling currents of over 500 amps at up to 1000 volts.

As mentioned before, SCR's are relatively easily turned on and remain conducting even after the gate signal is removed. Thus the

problem of turning the SCR off once it is in the conducting state seems to present itself as a major problem. An investigation of the literature presents one with various means of overcoming this problem.* Basically, they all consist of presenting the SCR with a reverse current of magnitude greater than the forward current. This reduces the current flowing through the SCR to zero, and the SCR is once again in a non-conducting state. This reverse current is usually provided by discharging a capacitor of sufficient size through the SCR.

The power supply, as built, can be broken down into two basic circuit areas: the high current circuit, and the triggering circuit. The high current circuit consists of the two available laboratory power supplies, the SCR's, and related high current components necessary for generating the high current wave form. The triggering circuit, on the other hand, is strictly a low current, low voltage timing apparatus, its purpose being to provide the SCR's with the correct gate signal at the correct time.

We first consider the high current components. Figure 2-5 is a block diagram of these components. The triggers for each SCR are shown for clarification. A diagram of the wave form is shown in the upper left-hand corner. The following time-event tabulation with reference to Figure 2-5 gives a general idea of the sequence of events.

---

*G. E. Silicon Controlled Rectifier Manual

Sequence of Events - Switching Circuit

Time	Event
$t = 0$	SCR 1, 2, 3, 4 Not Conducting
$t_1<t<t_2$	SCR 1 Conducting to E.C.M. load C_1 Charging V_L = (+)
$t_2<t<t_3$	SCR 2 Conducting to R_1 C_1 Discharges through SCR 1 turning it off. $V_L = 0$
$t_3<t<t_4$	SCR 3 Conducting to E.C.M. load C_2 Charging V_L = (-)
$t_4<t<t_1'$	SCR 4 Conducting to R_2 C_2 Discharges through SCR 3 turning it off. $V_L = 0$

At t_1, the cycle begins again.

Figure 2-6 is a schematic diagram of the SCR's and related components. For an ECM tool-workpiece resistance of less than 1 ohm, $R_1 = R_2 = 1$ ohm, $C_1 = C_2 = 100$ µf., and SCR 1, 2, 3, 4 are 100 amp. SCR's. The fuses shown are special fast-acting fuses which protect the SCR's from thermal overload. Figure 2-7 is a pictorial diagram of these same components. The SCR's are mounted on aluminum heat sinks, and provision is made for varying the load resistance and commutating capacitor values, depending on the ECM load. All internal connections are made via copper buss bar.

A 50 millivolt, 500 amp shunt resistor has been added in series with the E.C.M. load, and a 40,000 ohm voltage divider has been placed in parallel with the E.C.M. load. Thus the output current and voltage can be recorded simultaneously by a two channel Sanborn recorder. In addition, the current wave form is monitored on a C.R.O., which reacts fast enough to show any indication of arcing or other short duration changes in the current, that would not be recorded on the Sanborn.

For D.C. machining, the SCR switching circuits are bi-passed, and power is used directly from the high current sources. The same measuring and recording equipment is used.

We now consider the triggering circuit. One section of the circuit as originally built is shown in Figure 2-8. The complete triggering circuit consists of four identical units connected in series as seen in Figure 2-5. Each unit is a mono-stable multi-vibrator or "one-shot", and is triggered into action by a negative voltage change (-dV/dt) provided by the previous unit. Thus each in turn provides its corresponding SCR with the necessary gate signal to turn it on. Furthermore, each triggering circuit has its own time control consisting of an R-C combination. Thus the total cycle time is the sum of the time intervals of each unit set independently. This gives infinte variation of duty cycle and frequency as desired. With the components as shown in Figure 2-8 the upper frequency limit is 1000cps., but with certain minor changes can be raised to 4000 cps.

The circuits thus far described have been built and tested under conditions of a constant dummy ECM load. However, many difficulties arise when actual ECM testing is tried. The power supply is very unstable and extremely sensitive to load variation. Thus the actual ECM load, non constant and not entirely resistive, causes great instability. As the tool approaches the workpiece, the decreasing resistance will cause the SCR's to stop switching. This problem is partially overcome by placing a constant dummy load in parallel with the actual load. This helps somewhat, but not enough to permit a complete test under actual machining conditions. A constant series load was also tried with little success. While it eliminates arcing, it also eliminates the ability of the apparatus to stabilize itself by drawing extremely high currents momentarily if the gap begins closing.

Pulsed D.C. tests can be carried out using one side of the power supply, and two of the triggering circuits. Thus a series of these tests were carried out. Even though no actual negative pulses are provided by the power supply, the capacitive effect of the gap and some other circuit peculiarities causes negative current spikes to the extent that some tungsten carbide machining was possible.

The instabilities, for the most part, can be attributed to the triggering circuit. Sometimes more than 1 pulse travels in the triggering ring, and thus switches the SCR's at the wrong times. This results in feeding one power supply into the other and blowing fuses. Thus the triggering circuit was redesigned and the new circuit is shown in Figure 2-9. This circuit provides more uniform

pulses to the SCR's for better triggering. It is also assembled open ended. It is not a ring circuit as previously. Instead, the first "switch" is driven by a square wave generator. If an extraneous pulse is introduced, it only lasts for one cycle, since it has no place to go after the fourth SCR is triggered.

With all of the above modifications, the power supply still does not operate satisfactorily. It does provide pulsed D.C. to the varying ECM load with little trouble. With both positive and negative parts of the wave however, the slightest variation in load causes instability and blown fuses. The ultimate answer lies in further refinement of the triggering circuit, and perhaps a new design for the high current components.

2-4 DEVELOPMENT OF TOOL AND INSULATION:

Several different tool geometries and constructions, as well as several different insulations have been tried in the attempt to find a combination that will produce a good clean hole at high cutting rates with as little tool and insulation wear as possible. The basic requirements of a good tool are that it be fairly rigid, that it be impervious to the electrolyte and that it be reasonably simple to produce. The insulation must be strong enough to guide the tool in its hole if necessary without rupturing and thus causing a short circuit. It must also withstand the very high flow velocities and elevated temperature at the tool tip.

Tool Development:

The tool geometries are given in Figs. 2-10 and 2-11. Type AA was the first type of tool tried and was constructed of 1/4" o.d. x 1/16" i.d. stainless steel tube. The very thin wall under the insulation caused the tool to be very flexible, causing vibrations while machining. This often caused shorting and arcing which eroded the tool. The lip at the tool tip is unnecessary, usually shorting and eroding away. The rest of the tools were made without the lip. This tool, because of the very thin wall was difficult to construct so it was discontinued.

Tool type DD was turned from the 1/4" o.d. x 1/16" i.d. stainless steel tube with the dimension B = .100". This tool was quite stiff and was satisfactory. In order to further stiffen the tool it was stepped as in Type EE. Thus the tool could be lengthened without making it much more flexible. The section E does not drill and is necessary for tool holder -- work clearance.

Tool types BB and CC were made of brass with the straight tube soldered into the base. The bore is about one half of the tube diameter in these brass tubes. Tube sizes of 1/8" and 1/16" o.d. tools were used for the quantitative evaluation of the pressure chamber. In Appendix IV will be found the dimensions of the tools tried so far in this experiment.

Insulation Development;

Development of insulations followed a trial, evaluation, improvement patte n. The insulations are referred to by number in the rest of the report so we will give here the insulation numbers and descriptions.

Insulation 1: A red plastic insulation for use in electroplating work was tried. It did not adhere well and had no strength. The high speed flow peeled it off.

Insulation 2: Patching epoxy applied to the tool was lathe turned to uniform dimensions. It proved to be brittle and cracked off early in the E.C.M. process.

Insulation 3: Cotton thread was set in Dupont's Ducco Cement (accetate glue) and wound tightly along the tool. Its mechanical strength kept it intact but it burned through in several places.

Insulation 4: Saurisin glazing compound was tried but it cracked before it could be tested. Very brittle.

Insulation 5: Cotton thread was set in epoxy and wound tightly along the tool. It remained intact but burned off around the tip. Better than any previous tests.

Insulation 6: An aluminum tool of type DD was heavily anodized. The Anodizing was dissolved or worn away and the tool was badly corroded. Entirely unsatisfactory.

Insulation 7: Dynel thread was set in polyester resin and wrapped tightly around the tool. This turned out to be a good strong insulation. It seldom burns through but it does usually chip or burn away for about 1/32" or 1/16" from the tip. This is the best insulation that we have tried, but it still does not give us the really constant tip geometry that we need for consistent results and ultra high feed rates. This insulation was used on all of the quantitative pressure chamber evaluation tests.

Insulation 8: Fiberglass fiber was set in polyester resin and wrapped tightly around tool. To get a smooth surface this was smoothed up and given a second coat of resin. The results were similar to Insulation #7 but the insulation is thicker than the Dynel of #7 and has a greater tendency to burn through. Insulation #7 is superior.

Insulation 9: Attempts have been made to bond a glass tube over the electrode. We have not yet satisfactorily bonded the glass to the electrode but are investigating various bonding media.

Further trials should also be made with substances such as the ceramic coatings used in rocket nozzles. Such coatings have to withstand conditions of similar nature but much more extreme than those encountered in E.C.M. work.

Chapter III

DRILLING TESTS IN PRESSURE CHAMBER

3-1 THEORY:

The basic ECM theory is quite simple. If we immerse two electrodes in an electrolyte and pass a current, the positive electrode (in the case of a metal) will be machined away. The amount of metal removed is determined by Faraday's law for electrical work which states that if we pass 96,000 coulombs (amp-sec) of charge we will alter (ionize) one gram equivalent weight of material divided by the charge of the ions produces. Iron can take on the valences of +2 and +3. There are many possible reactions with the conditions encountered in electrochemical machining so we can only say that the average value of the valence is between +2 and +3.

The equation for the removal rate of iron is thus;

$$M = \frac{4.6 \times 10^{-3} I}{Z} \qquad (3\text{-}1)$$

M = Machining rate (in.^{3}/sec.) removed

I = Machining current (amperes)

Z = Average valence of Ions removed

Test #11 (Appendix II) was a good test so the hole volume was measured and the integrated I x t (time = t) were taken from the recorder chart. The above equation (3-1) showed the average valence of the ions removed to be 2 5+. This is in good agreement with the above theory.

From the basic theory we see that to increase metal removal rates we merely need to increase the current. If we are drilling a straight hole and assume the cutting to take place only at the bottom of the hole, the drill feed rate is determined by the current density at the bottom surface independent of drill diameter. If the cutting area is doubled, current must be doubled to double the material removal rate and thus hold the feed rate constant. Thus we can study the behavior of small diameter drills and extrapolate to larger drills.

Since feed rate is dependent on current density, our object is to increase current density as far as possible. There are several factors that limit current density. There is a large amount of heat produced in the cutting zone. If we assume the total voltage drop is across the tool-work gap (a fairly safe assumption) the heat released in the cutting zone is the product of voltage and current (watts). If this heat is sufficient to cause the electrolyte to boil, the conducting electrolyte film is destroyed, the feed closes the gap, and the tool shorts or arcs interrupting the machining process. Therefore the electrolyte flow must be sufficient to carry away the heat produced without

exceeding its boiling point. From this theory it is possible to calculate a relationship between flow rate and voltage x current for aqueous electrolytes.

$$F_M = \frac{1.55\ VI}{(T_b - T_o)} \tag{3-2}$$

F_M = Minimum flow to dissipate heat without boiling (in^3/min)

V = Machining voltage

T_b = Boiling temp (deg F) at chamber pressure

T_o = Supply electrolyte temperature (deg F)

I = Machining current (amps)

We can define a coefficient of cooling C_c by the equation;

$$C_c = \frac{1.55\ VI}{F(T_b - T_o)} \tag{3-3}$$

we expect boiling if this coefficient is greater than 1. In our tests however, the highest values of C_c obtained were .30. At these points there was arcing and often instability of flow.

This brings us to another limitation, that of cavitation. We have a thin tube with very high velocity flow in it. This produces a decrease in pressure (Δp) predicted approximately (if we assume inviscid flow) by Bernoulli's flow equation $\Delta p = \rho V_f^2$ where we assume that the supply velocity, at the gauge where p_g is measured, is zero. (V_f is the flow velocity in the tool)

An additional pressure decrease occurs at the tip of the tool where the flow turns abruptly to rise up the sides of the tool out

of the drilled hole. There is a strong radial pressure gradient due to streamline curvature.

If we again assume inviscid flow (a very good approximation at these high flow velocities) the pressure gradient is predicted approximatly by; $dp/dn = \rho V_f^2/r$, n being a unit vector perpendicular to the streamlines and r the radius of curvature of the streamlines at the point being studied For our approximation we will assume the geometry shown in Figure 3-1.

If we assume that the flow velocity V_f is constant across the section A-A (i.e. for all $r_i<r<r_o$) the following integration gives the expected pressure difference from r_i to r_o.

$$p_o - p_i = \rho V_f^2 \int_{r_i}^{r_o} dr/r = \rho V_f^2 \ln (r_o/r_i) \qquad (3\text{-}4)$$

Since $V_f = F/(\pi D(r_o - r_i))$ we can write;

F = Volumetric flow

$$p_o - p_i = \left(\frac{F}{\pi D(r_o - r_i)}\right)^2 \rho \ln (r_o/r_i) \qquad (3\text{-}5)$$

This is quite approximate, but will give an idea of the pressure difference expected from r_o to r_i.

The pressure at r_i is approximately the supply pressure (at the tool pressure gauge) minus the Bernoulli pressure drop calculated at section A-A and 1/2 the pressure drop due to streamline curvature.

$$p_i = p_g - \frac{\rho}{2}\left(\frac{F}{D(r_o - r_i)}\right)^2 \left(1 + \ln\,(r_o/r_i)\right) \qquad (3\text{-}6)$$

p_g = gauge pressure of slow moving fluid just before it enters tool.

If the pressure at r_i is less than the vapor pressure of the electrolyte at the temperature to which it has been heated by the reaction, cavitation can occur.

This gives us the basic theory, but is insufficient to make any accurate feed limit predictions as we have at this point only a poor idea of what the accurate geometry of the cutting zone actually is. The gap width below the tool is very critical in these calculations.

We can now define a more useful coefficient of cooling as follows;

$$C_{cr} = \frac{1.55\ VI}{F\ (T_{br} - T_o)} \qquad (3\text{-}7)$$

In this case, T_{br} is the boiling temperature at the reduced pressure given by equation (3-6). If C_{cr} is less than 1 we would expect to find no boiling.

3-2 1080 STEEL (40 VDC):

The first tests were run in the plexiglas tank at atmospheric pressure. Under these conditions it was possible to observe the flow around the tool as it entered the work. Through trial and error it was discovered that at voltages above about twenty volts much arcing occurred, destroying the tool and insulation and producing a wide,

irregular hole. If the voltage was kept between fifteen and twenty volts the best results were obtained. The most critical point was just when the tool entered the surface of the workpiece. If the feed was above the lowest feed rate of .079"/min. the tool would often arc and sometimes make contact and completely short circuit. During one of the tests it was noticed that the arcing was occurring only during the high pressure portion of the pump cycle, i.e., when the flow was at its maximum value. It was reasoned that the flow was probably cavitating as it turned the corner at the bottom of the tool. These pockets where the electrolyte was discontinuous caused the reaction to stop causing the gap to decrease until an arc jumped the gap eroding the tool and workpiece.

A second mechanism that is caused by cavitation or other flow instabilities is a high frequency vibration of the flexible tool in its hole causing arcing at the points where it comes too close to the edges of the hole. These two mechanisms probably account for the rapid tool wear, arcing, and high pitched squeal often found when the tool enters the work. The squeal makes the condition easy to recognize.

The problem of cavitation could generally be solved by reducing the electrolyte flow rate to a fairly low flow. These low flow rates limit the feed rates to the previously mentioned values of about .079"/min. because of the cooling problem.

After the tool penetrates a reasonable depth (about 3/8 in.) into the workpiece, the flow rate and feed rate can be substantially increased. Conditions improve with depth. With maximum pump pressure (about 3,000 psi.) and a very deep hole with small clearances, a feed rate of .55"/min. was once obtained. We were not able to reproduce this condition however.

It was reasoned that the deep hole essentially pressurizes the cutting zone due to the flow resistance in the fluid path out of the hole. The pressurization both raises the boiling point of the electrolyte and stabilizes the flow by reducing or stopping cavitation. Thus we reasoned that an increase in pressure should stabilize the flow making higher flow rates possible. The increase would also raise the boiling point of the fluid thus greatly increasing the capability for carrying heat away from the cutting zone.

At this point testing was stopped and a pressure chamber for pressures up to 5,000 psi. was constructed. The design of the chamber is described in the section of "Equipment" and detail drawings appear in the appendix.

The first tests in the chamber were at 2,000 psi. and 20 volts. Under these conditions the current drawn was very small (only about 15 amps) and the process soon shorted out at the very low feed speed of .157"/min. It was decided to try higher voltages and runs were made at 40, 60, and 80 volts. All showed a marked improvement over 20 volts and it was decided to start testing the process at 40 volts. Higher voltage tests will be discussed later.

A series of tests were run in the pressure chamber using chamber pressures from 0 to 3,000 psi. The voltage was held at 40 and the flow was held as near 130 $in.^3/min.$ as possible. The results of these and all other tests in the chamber are shown in Appendix II. The results of the pressure tests are shown in Figure 3-2. The curves show limiting entry feeds and limiting feeds when the tool is at least 3/8" into the work. The data points consist of points where the process failed (above the limit), and points where the process operated smoothly (below the limit). In some cases, conditions that appear to be limiting were found in which the process would arc occasionally but would work well most of the time. This system is used for both curves. Very low "above the limit" tests were considered less reliable than higher "under the limit" tests as a low point could and often was caused by insulation failure which was not the effect we are looking for in this plot. It is unlikely that an accident will cause a very high point.

The high pressure end of the entry rate curve is poorly defined, as a rate high enough to find entry failure destroys the usefulness of the rest of the test.

From the graph it can be observed that the pressure chamber is very effective at increasing feed rates at 40 volts electrode potential. It appears that 1500 to 2000 psi. is adequate to gain most of the improvement possible at 40 volts and 130 $in.^3/min.$ flow rate. More data points at higher pressures are necessary. By increasing the supply of air pressure to our pump, we can theoretically

raise our peak pressures to 5000 psi. This will be investigated in future work.

We feel that this improvement due to pressure comes from two main effects. The most important seems to be the stabilization of the flow at high flow rates. Cavitation is suppressed, improving the quality of the electrolyte layer between the electrode and the workpiece and eliminating high frequency oscillations of the flow and tool. These oscillations were a major cause of arcing due to variation of the machining gap. The increased flow decreases heating in the cutting zone and keeps the electrolyte below its boiling point.

The second effect is the increase in the boiling point due to the pressure. The change from 14.7 to 2500 psi. increases the boiling point from $212^{\circ}F$ to $668^{\circ}F$, an increase in heat transfer capability of about five times. (Assume $T_o = 100^{\circ}F$)

In this series of tests, we were unable to obtain cooling coefficient values greater than 3/10 without arcing. This is due to the Bernoulli reduction in pressure and the streamline curvature pressure gradient mentioned in the section on Theory. This reduced pressure lowers the boiling point correspondingly and produces cavitation if the pressure gets below the vapor pressure. Figure 3-3 shows the pressure reduction due to this effect when using a 1/16" o.d. x 1/32" i.d. tool (#4) giving a value of D = 3/64" and assuming the flow to be 130 $in.^3/min.$ (also assuming the geometry given in the section on Theory).

From Figure 3-3 we see that the pressure reduction is a very strong function of gap size. For the high pressures such as 2000 psi. where we often operate the chamber, the pressure reduction is approximately the pressure required to suppress cavitation. We think that our machining gaps are in the order of .002" so this pressure reduction effect may well be a main controlling factor. The great improvement encountered in increasing voltage may be due to the fact that a higher voltage will cause the process to operate with a wider gap thus reducing the pressure reduction and possibly moving the process into a non-cavitating region. (An increase in voltage allows the process to draw the necessary current for a given feed rate across a wider gap).

When the feed is increased, a higher current is necessary, causing a narrower gap at the same potential. By further increasing voltage, a wider gap can again be stabilized, allowing still higher feed rates. By carefully balancing flow rates with cooling requirements, and increasing voltage we should be able to greatly increase machining rates. We must improve our insulations to combat the increased temperatures and voltages however.

We can thus conclude that as we expect, machining rates can be substantially increased by pressurization of the cutting process.

One problem that was encountered in pressurization of the process is that the tool holder acts as a piston in the pressure chamber, loading the milling machine with about 2500 pounds force at 2500 psi. chamber pressure, as the piston has an area of about

1 in^2. The problem arises when the pressure in the chamber fluctuates due to pumping oscillations or drops due to the sudden flow reduction and the lag time of the regulator in such a stiff system. The machine deflects about .015" for a pressure difference of 3000 psi. Thus if we lose pressure from 3000 to 0 psi. during machining, the machine will return to equilibrium position closing the machine gap by about .015". This generally creates a dead short!

The situation is basically somewhat unstable as a decrease in gap causes a decrease in flow decreasing pressure which causes a further decrease in gap width. The stabilizing factor is that a decrease in gap size increases machining rate. However the variation of machining rate is much smaller than the rate of gap fluctuation so we get a difficult situation to control. There are several ways of overcoming this problem. The first one is to regulate pressure more accurately, reducing fluctuations. We have done this by improving our use of the throttling valves and pressure regulator. The machine stiffness has been increased by shortening the overarm overhand by moving the chamber closer to the vertical machine ways. Both of these measures have greatly improved the situation. The gap length fluctuations can be observed in the milling current trace. The current varies inversly with the gap length so the trace shows the frequency of gap oscillations and the severity of the amplitude.

The greatest improvement can be made by reducing the piston size of the tool holder and increasing the accumulator size to reduce pumping pressure oscillations. These will be done in future work.

Part of the improvement from increased voltage may be due to the increase in machining gap and the corresponding decrease in sensitivity to gap length fluctuations. However, it is interesting to note that pressurization of the chamber, even with its decrease in gap precision greatly improves the cutting process. Elimination of pressure fluctuations will further improve the process.

Some of the holes drilled are shown in Figure A7-10. The somewhat conical appearance of the test 3 hole is due to the low feed rate and the loss of insulation at the tool tip. The tighter more accurate dimensions of tests 5, 11, and 20 are due to better insulation conditions at the tool tips and higher feeds. The increase in hole diameter at the bottom of hole #5 was caused by stopping the feed a short time before stopping the current. Test #8 was made with a larger tool. The increased diameter bands are the points where the feed was stopped while shifting to a higher feed rate. Test #20 was drilled with a high feed rate (.71"/min.) which, along with the good insulation explains the very tight accurate hole. The tools used in drilling the holes are shown with the holes.

3-3 1080 STEEL (80 VDC):

Tests were carried out at 80 VDC in the pressure chamber with a NaCl electrolyte. It was thought that an increase from the previous 40 to 80 volts would increase the tool-workpiece gap. This would make the process less sensitive to fluid pressure fluctuation and tool vibration.

For most tests the tool pressure was maintained above 2800 psi, and the chamber pressure above 2000 psi. As suspected, the maximum feed rates can be increased over comparable 40 volt tests.

	40 Volts	80 Volts
Max. Entry Feed Rate (in/min)	0.275	0.275
Max. Feed Rate (in/min) (Tool at least 3/8 inch in workpiece)	0.71	1.53

It is noted that no increase can be made in entry feed rate. The maximum rate, with the tool at least 3/8 inch into the workpiece, can be more than doubledwhen the voltage is doubled. The difficulty in starting a hole is to some extent due to the fact that the workpiece sits in the electrolyte for a relatively long period of time before any substantial metal removal takes place. A passive film probably builds up to a much greater thickness than does during the actual drilling process while the drill sits above the workpiece. Also, once into the workpiece, the flow is much more restricted since it has to travel up the side of the tool. This

probably has certain stabilizing effects on the process which in part account for higher feed rates. This in itself leads to the conclusion that higher entry rates can most easily be achieved by clamping a collar on top of the workpiece, providing the tool with a ready made entry hole. This idea has not yet been tried, but shall be at a future date.

It is especially interesting to note that current densities ranging from 13,000 to 19,700 amps/in^2 are achieved for feed rates in the range of 1.5 in/min. Most of the literature on ECM gives maximum densities in the range of 2000 amps/in^2. Essentially the increased rates achieved here are due to two main effects, pressurization of the process, and a voltage increase to 80 over the normal 12-16 volts of commercial ECM equipment.

3-4 TUNGSTEN-CARBIDE:

Various attempts were made at drilling tungsten-carbide using both NaCl and NaOH electrolytes. All tests were conducted in the pressure chamber with the tool electrolyte pressure greater than 2600psi., and the chamber electrolyte pressure greater than 2000 psi. The main variable was originally to be the current wave shape and frequency as explained in the section on the power supply for the removal of the passive film. However, the difficulties encountered with the power supply made it impossible to ever complete a test with both the positive and negative portions of the wave present.

A number of tests were carried out with a positive D.C. square wave at various frequencies and with current spikes both positive and negative as provided by a capacitor discharge and circuit transients. These techniques are explained in more detail in conjunction with their respective tests

The first tests were with a NaCl electrolyte. A positive amplitude square wave of 50 cps with an 8:1 duty cycle was tried. Holes were obtained but much arcing occurred at the gap. From the rough appearance of the holes, and the CRO arcing indication, it is concluded that they were probably made by a sparking process in conjunction with the ECM process. Voltage was increased for a wider gap in hopes of reducing the arcing. Also a 20 uf. capacitor was connected across the gap to produce current spikes with each cycle of the square wave. However, this seemed to increase arcing. Most of these tests were failures. The frequency was increased to 1000 cps. and other rough holes were obtained. All of these tests were at a feed rate of 0.079 inch/min. The results indicate that little improvement, if any, seems possible with the NaCl electrolyte and a tungsten-carbide workpiece.

The remainder of the tungsten-carbide drilling tests were carried out in NaOH electrolyte. Again various frequency positive amplitude square waves were tried, both with and without a capacitor across the gap. Results were for the most part better than those obtained with the NaCl electrolyte. The best results were obtained using a square wave with a frequency of 1000 cps. and a 2:1 duty cycle.

A small negative transient was present in each cycle and this was probably the main factor in limiting the passive film build up. The results are best summarized as follows:

Feed Rate (in/min)	Current Density (amps/in^2)	Finish
0.079	940	excellent
0.098	1890	rough

There is probably a relationship between the frequency of the current pulses and the maximum rate at which material may be removed. The greater the feed rate, the faster the film build up due to the higher current. This in turn necessitates more frequent negative pulses for the film removal. While at the 0.079 in/min feed rate the test ran smoothly and yielded excellent results, the 0 098 in/min test was a limiting test under conditions of identical wave form.

There is certainly much room for further testing at higher frequencies and with better defined negative pulses. The power supply has not yet operated as it was designed to. The testing thus far does warrent continued work in this area.

3-5 INCONEL 600:

Forty volt D.C. drilling tests were carried out using a NaCl electrolyte. These tests yielded the following maximum feed rates:

Entry Feed Rate (in/min)	Max Feed Rate (in/min)	Current Density ($amps/in^2$)
0.275	0.71	8200

These rates and current densities are about the same as those obtained in 1080 steel under similar test conditions. The main noticeable difference being a much closer fit between the side of the tool and the workpiece as compared to the 1080 tests. This reduced area causes a considerable decrease in flow during testing. The most successful tests are obtained by removing 1/16 of insulation from the tip of the tool. This allows machining to take place at the side of the hole as well as directly under the tool, thus giving the desired flow clearance.

NaOH was tried unsuccessfully as an electrolyte for this alloy. With NaCl under D.C. conditions Inconel 600 can be machined as easily as 1080 steel with ECM.

3-6 STELLITE J:

Again tests were conducted in the pressure chamber using an NaCl electrolyte and 40 VDC. This time rates were lower than the corresponding 1080 steel tests. Pulsed DC (750 cps) with negative transients yielded rates somewhat higher than the D.C. rates. As in the Inconel tests the tool-workpiece side clearance was small and removing 1/16 inch of insulation was necessary for successful testing. Again NaOH proved unsuccessful as an electrolyte.

Voltage	Entry Feed Rate (in/min)	Max Feed Rate (in/min)	Max Current Density (amps/in^2)
40 VDC	0.218	0.433	7,400
40 V (750 cps)	0.157	0 55	10,200

3-7 SUMMARY OF DRILLING TESTS:

The following is a tabulation of the maximum feed rates and current densities for the four materials tested. While the 1080 steel, Inconel 600, and Stellite J may be approaching maximum limits in feed rates, the tungsten-carbide rates are far from what they should be. The answer most likely lies in perfecting the power supply.

Summary of D.illing Tests

Material	Entry Feed Rate (in/min)	Max Feed Rate (in/min)	Max Current Density (amps/in^2)
1080 Steel	0.275	1.53	19,700
Tungsten-Carbide	0.098	0.098	1,890
Inconel 600	0.275	0.71	8,200
Stellite J	0.218	0.55	10,200

Chapter IV

MOLTEN SALT ELECTROLYTES

Thus far, one of the main factors limiting the rate of material removal has been the formation of insoluble surface films on the anode. It is known that the rate at which the machined surface moves inward (the machining velocity) is directly proportional to the current density (amps/in^2) The insoluble oxides, sulfides, etc that form at the anode surface limit the current density. The metallic ions of the material being removed must diffuse through this film, and according to Ficks Law of diffusion, the rate is inversely proportional to the film thickness. Furthermore, it is known that the diffusion constant depends on the absolute temperature such that increasing the temperature increases the diffusion rate

The information contained in the above paragraph plus the fact that chemical reaction rates in general can be increased by increasing the concentration and temperature of the reactants led to the concept of using a molten salt as the electrolyte in the E.C.M. process The concentration of a molten (fused) salt is by definition higher than the same salt in an aqueous solution, and the melting temperatures of such salts as might be used for machining are extremely high when compared to the boiling temperature of water both at atmospheric and elevated pressures (Fused Salt Data, Appendix I)

Initial tests were run using steel drill rod electrodes in a bath of $ZnCl_2$. The experimental set-up was similar to that shown in Figure 4-1. The electrodes were immersed in a bath of molten $ZnCl_2$, a voltage was impressed across the gap, and current was allowed to flow for a specified time interval. The electrodes were weighed before and after the test to ascertain the weight loss. These initial tests exhibited the expected trend. Current densities could be increased over similar aqueous solution experiments. Machining in $ZnCl_2$ however, deposited a heavy zinc plating on the cathode. $ZnCl_2$ was, therefore, not a good choice for an electrolyte.

Some consideration was given to choice of anode material and appropriate salts before continuing. Since tungsten carbide has exhibited such low rates of material removal it was decided to use tungsten carbide as the anode material exclusively. An examination of various literature on E.C.M. shows that among the many non-plating electrolytes, aqueous solutions of NaCl, NaOH, $NaNO_2$, and KCl have all been used successfully in machining various materials. An investigation of the melting temperatures of these salts (Appendix I - Fused Salt Data) yielded the fact that both NaCl and KCl have unreasonably high melting temperatures (1400°F) and would probably be very limited in application. NaOH and $NaNO_2$ on the other hand have melting temperatures in the range of 550°F, which is not an unreasonable temperature to work with It is fortunate that NaOH is in this range, since it has already been

proven somewhat successful in aqueous solution as an electrolyte for tungsten carbide.

With the apparatus as in Figure 4-1 a series of forty tests was conducted, using the various aforementioned salts both in aqueous solution and in the molten state. These tests were carried out at constant voltage while the time of test, current flow and anode weight loss were recorded. In addition the depths of immersion of the electrodes in the electrolyte were recorded since they varied slightly for each test. This data is compiled in Appendix I. The temperatures of the various tests were held constant for a particular salt, as given in the temperature data, and all aqueous solution tests were at approximately 80°F. The testing procedure was simply to immerse the electrodes, apply a 5 volt potential for a time interval, and record the pertinent data.

The first set of curves of interest are seen in Figure 4-2. Weight loss per unit depth of immersion is plotted against time. (The unit depth factor is included, since the electrodes were not all immersed to the same depth.) These curves clearly show that fused NaOH is the superior electrolyte of all those tested. In fact, NaCl (20% solution by weight), $NaNO_2$ (Fused), KCl (20% solution) and Zn[illegible] solution) exhibited such small weight losses under the same conditions they could not be plotted on this figure. We note also that while the lower curves flattened out with time, the NaOH curve has constant slope indicating a constant rate of weight removal; $\Delta W/\Delta t$ is constant. Let us examine these data by considering

Faraday's Law:

$$W = \frac{I\ t\ A}{ZF_o} \qquad (4\text{-}1)$$

where: W = weight (grams)

I = current (amps)

t = time (seconds)

A = atomic weight (grams)

Z = valence of anode

F_o = constant = 96,500 amp-seconds

We rearrange the equation to the form:

$$\frac{W}{I\ t} = \frac{1}{F_o}\ \frac{A}{Z} \qquad (4\text{-}2)$$

where $1/F_o$ and A/Z are constants. Since tungsten carbide consists of tungsten and carbon held together with a cobalt binder it is not a matter of looking up the values of A and Z in a handbook. However, an A/Z equivalent can be computed from the experimental data. It must be remembered that this is very unlikely that true value of A/Z for what ever reaction might be taking place at the anode, since limiting surface films are probably still present.

In figure 4-3 weight loss is plotted against current times time, and from this plot we obtain the slope of 1.33×10^{-2} grams/amp minute. By equation (4-2);

$$1.33 \times 10^{-2} = \frac{1}{F_o}\ \frac{A}{Z}\ \frac{\text{grams}}{\text{amp-min.}}$$

or

$$\left(\frac{A}{Z}\right)_{equiv} = 21.4 \text{ grams}$$

With these values established, we can consider another form of Faraday's Law:

$$v = \frac{j}{454\ \gamma} \left(\frac{A}{F_o Z}\right) \qquad (4\text{-}3)$$

v = rate at which machined surface moves inward (inch/minute)

j = current density (amps/in^2)

γ = density material being removed (lb/in^3)

$\frac{A}{F_o Z}$ = constant (grams/amps-minute)

454 = (grams/lb)

If we take γ as a density of tungsten carbide we thus have an equation relating v and the current density. (γ should be the density of the reacting element at the anode, but since this is unknown at present, the density of tungsten carbide is used as an approximation.) Thus a determination of the maximum current density gives an indication of the maximum rate at which the machined surface moves inward

In the original fused salt experiments as shown in Figure 4-1, the electrodes were widely spaced (0 75 inch) and of approximate surface area 0.1 in^2. Since the current densities desired are in the range of 10 - 10^3 amps/in^2 this apparatus would require a power supply for beyond that available. The best alternative

was to reduce the area of machining to reduce the total current and also to reduce the gap so that lower voltage could be used to force the current through the gap.

The final configuration was as shown in Figure 4-5. The anode was coated with an insulating material capable of withstanding the high temperatures involved (Sauereisen cement). Only the flat circular end of the anode was exposed to the electrolyte. The gap was set at approximately .01 inch with a thickness gage. The voltage across the gap was then increased and the corresponding values of current were observed. Typical data gave results as shown in Figure 4-4. The current asymptotically approaches a maximum value at higher and higher values of voltage.

Fused NaOH yielded a maximum current density of 1200 amps/in^2. This compared with 388 amp/in^2 for $NaNO_2$ and 318 and 95 amps/in^2 for aqueous solutions (20% by weight) of NaOH and $NaNO_2$ respectively. Inserting this value (1200 amps/in^2) into equation (4-3) along with the appropriate constants we obtain the maximum machining velocity:

$$v_{max} = 0.065 \text{ inch/minute}$$

At first glance, this figure seems low. However, this is a rate for zero fluid velocity and at atmospheric pressure. In this context, this figure becomes much more meaningful. It compares with the rate of 0.08 inch/min which was obtained with a 20% by weight solution of NaOH in the pressure chamber and through the use of pulsing current. It is further noted that drilling steel

at atmospheric pressure produced drilling rates of less than 0.1 inches/minute. Thus it seems that under pressurization and with high enough fluid velocities, it should be possible to drill tungsten carbide at rates greater than 1 inch minute using a fused NaOH electrolyte and D.C. power.

It can be concluded that fused NaOH is a good electrolyte for the machining of tungsten carbide. It is also of interest to note that the surface finish obtained is uniform and smooth with the fused NaOH. This is in contrast to the rough pitted surface obtained with fused $NaNO_2$.

Chapter V

LASER TESTS

Tests were conducted to determine whether high intensity electromagnetic radiation (light) from a laser has any effect on the E.C.M. process. It was thought that in machining materials which form insoluble surface oxides or other such "tough" surface films, the laser light might be a means of continuously breaking up the film as it builds up. Tungsten carbide is such a material.

Devising a means for directing laser light into the pressure chamber would not be necessary for the initial investigation of the laser's effect. Furthermore, for hole drilling operations in general, directing laser light to the area of machining would certainly pose serious problems. However there are enough surface forming operations possible with E.C.M. that would allow the laser light to fall directly on the machining surface. With this in mind, a simple electrolytic cell was decided upon as the best apparatus for this investigation.

Figure 5-1 is a diagram of the cell and related apparatus. The laser used in the investigation was a ruby laser capable of providing high energy light pulses of short duration. A brief description of this laser and its operation is contained in Appendix III. The experimental procedure consisted of applying a constant voltage to the cell and then

observing the change, if any, in current through the cell when a pulse of laser light was incident on the anode surface

Initial tests of a tungsten carbide anode and steel cathode in both NaOH and NaCl electrolytes proved negative. These tests were tried for various laser light intensities varying from a 1/8 inch spot of light down to the sharpest focus attainable with the laser's optical system.

Since the laser light was incident on such a small fraction of the entire anode surface, the next step was to coat the entire tungsten carbide anode with an insulating material (microstop lacquer) with the exception of a small portion just large enough to completely block the path of the pulse of laser light Again no effect was observed for either electrolyte or for various intensities of laser light.

It was observed that the laser light was diffused by the violent bubbling action that takes place at the electrodes during the electrolytic action. The most concentrated pulse of laser light attainable from the apparatus, capable of actually melting the tungsten carbide surface under zero current conditions in the cell, could not penetrate this bubble layer

From the above results, it seems highly improbable that laser light could ever be used successfully to break up the surface films that form during the machining process. It is true that pressurizing the entire E.C.M. operation substantially reduces the volume of bubbles formed, but this poses the aforementioned

problems of directing laser light into a pressure chamber. Furthermore, even if the laser light could be directed at the pressurized process, the high velocity fluid containing sludge and metal particles would probably still diffuse the laser light enough to make it ineffectual at the anode surface.

Chapter VI

CONCLUSIONS

Conclusions have been drawn at the end of the foregoing sections. However, it is worthwhile to summarize them here.

1. In drilling, high rates can be obtained if sufficient hydrostatic electrolyte pressure is maintained in the active ECM zone There are four primary effects of pressurization:
   a. Elimination of boiling
   b. Increase of electrolyte conductivity and diffusion rates due to higher temperature.
   c. Suppression (by dissolving) of hydrogen bubbles.
   d. Elimination of electrolyte cavitation
2. In high speed drilling, it is essential to employ a "starting sleeve" in order that the flow and pressure conditions are established before machining starts.
3. When the above pressure conditions are maintained, steel can be drilled at feed rates as high as 1 1/2 in/min at current densities approaching 20,000 amps/in^2. Operating voltages of the order of 100 volts are required.

4. Pulsed DC current, having short reverse polarity "spikes" appears quite promising for machining materials such as tungsten carbide which are normally very difficult to work by ECM. More work is required before we can give positive conclusions relative to this mechanism.

5. Fused salts appear to be effective in ECM. Clearly they permit high temperature diffusion within anode layers such as are formed on tungsten carbide. Fused NaOH produced current densities of almost 1000 amps/in^2 when machining tungsten carbide in a "static" (no flow, no pressurization) test.

6. Under pressurized conditions, Stellite J and Inconel 600 were machined at 0.55 and 0.71 in/min respectively.

7. The use of laser energy for removing reaction layers on the anode was completely ineffective. The primary reason appears to be the diffusion of the light by the bubbles in the electrolyte.

RECOMMENDATIONS

We strongly urge that follow-up work be carried out in three highly promising areas:

1. We should determine more fully the relationships between maximum feed rate and the pressure-flow-temperature conditions within the active ECM zone. While we have achieved high rates, we do not consider them to be maximum.

2. We should explore various pulse shapes and frequencies in order to determine whether this method will or can remove anodic layers without producing significant tool wear.

3. Various other "low temperature" fused electrolytes should be studied, and a simple drilling test rig utilizing fused electrolyte, should be built and tested.

Chapter VII

ACKNOWLEDGEMENTS

The authors wish to express their thanks to the U. S. Army Materials Research Agency, Watertown, Massachusetts, for sponsoring the project, and especially to Mr. Harold B. McNamara, technical supervisor, for his help and guidance in carrying out the project. Secondly, the authors wish to express their appreciation for the professional help of Messrs. John Leach, F. H. Anderson, R. J. Bowley, Ralph Whittemore, and Jared J. Wolf in the building and testing of the equipment. Dr. P. Narayan Nayak and Mr. F. P. Gerstle Jr. deserve special mention for their help in designing the equipment and carrying out experiments. Further thanks are due Mr. C. Mpagazehe for the construction of the tools and Miss Kathleen M. Carney for typing the manuscript.

Appendix I

FUSED SALT DATA

Electrolyte Data:

Electrolyte	T (melt) °C	T (boil) °C	20% Aqueous Solution (by weight) lb/gal
NaCl	801	1413	1.91
NaOH	318	1390	2.04
$NaNO_2$	271	320	1.90
KCl	776	1500	
Z_NCl_2	262	732	1.98

Temperature Data:

Electrolyte	Temperature of Test °F
All Aqueous Solutions	80
NaOH (Fused)	900
$NaNO_2$ (Fused)	750

FUSED SALT DATA

Maximum Current Density Data:

Electrolyte	Max. Current (amps)	Area (in^2)	Current Density amps/in^2
$NaNO_2$ (Fused)	1.10	2.83×10^{-3}	388.
$NaNO_2$ (20% Soln)	0.27	2.83×10^{-3}	95.4
NaOH (Fused)	3.5	2.83×10^{-3}	1240.
NaOH (20% Soln)	0.9	2.83×10^{-3}	318.

Anode Matl. = Tungsten Carbide rod D. = 0.060 inch

Cathode Matl. = Steel drill rod D. = 0.625 inch

Cap Width = 0.010 inch

Maximum voltage = 20 volts

Typical Current values as the voltage increased: (NaOH 20%)

Volts	Amps.
6	0.50
8	0.80
10	0.90
12	0.90
14	0.90
16	0.90
20	0.90

FUSED SALT DATA

Anode Tungsten Carbide Rod (1 through 27) D ± 0.050 Inch (28 through 40) D = 0.060 Inch

Cathode Steel Drill Rod 0.0625 D

Voltage 5 V.D.C. (constant)

Temp. (as in Temp. Data)

Test No.	Electrolyte F=Fused S=Solution	Time (Min)	Current (amps)	Immersion Depth (Inch)	Area (In^2)	Current Density ($Amps/In^2$)
1	NaOH (F)	2.0	4.5	0.54	0.083	54.3
2	NaOH (F)	1.0	4.8	0.59	0.091	52.8
3						
4	NaOH (F)	3.0	4.7	0.64	0.068	69.4
5	$NaNO_2$(F)			0.69		
6	$NaNO_2$(F)	1.0	2.5	0.58	0.0895	28.0
7	$NaNO_2$(F)	2.0	3.0	0.62	0.0955	31.4
8	NaOH (S)	2.5	2.0	0.73	0.112	17.9
9	NaOH (S)	1.0	2.0	0.74	0.114	17.6
10						
11	$ZNCl_2$(F)	2.0	0.9	0.64	0.985	9.15
12	$ZNCl_2$(F)	1.0	0.5	0.65	0.100	5.00
13	$ZNCl_2$(F)	3.0	0.8	0.82	0.126	6.35

FUSED SALT DATA (cond't)

Test No.	Electrolyte F=Fused S=Solution	Time (Min)	Current (amps)	Immersion Depth (Inch)	Area (In^2)	Current Density ($Amps/In^2$)
14	NaCl (S)	1.0	Neglig	0.76	0.177	
15	NaCl (S)	2.0	0.02	0.80	0.123	0.163
16	$ZNCl_2$(S)	1.0	0.1	0.93	0.143	0.700
17	$ZNCl_2$(S)	2.0	0.06	0.98	0.151	0.398
18	$NaNO_2$(S)	1.0	0.2	0.83	0.128	1.56
19	$NaNO_2$(S)	2.0	0.1	0.90	0.139	0.720
20	NaOH (S)	3.0	2.3	0.92	0.142	16.2
21	NaOH (F)	4.0	4.0	0.68	0.107	37.4
22	NaOH (F)	1.0	5.0	0.65	0.100	50.00
23	NaOH (F)	4.0	4.5	0.59	0.091	49.5
24	$NaNO_2$(F)	3.0	2.3	0.65	0.100	23.
25	$NaNO_2$(F)	1.0	2.4	0.63	0.097	24.8
26	$NaNO_2$(S)	4.0	0.2	0.77	0.199	1.69
27	NaOH (S)	4.0	1.6	0.73	0.112	14.3
28	NaOH (F)	0.5	6.8	1.17	0.220	30.9
29	NaOH (F)	1.0	7.1	1.10	0.206	34.4
30	NaOH (F)	1.5	6.0	1.02	0.192	31.2
31	NaOH (F)	2.5	6.8	1.08	0.203	33.5
32						
33	NaOH (F)	4.0	6.65	1.115	0.216	30.8

FUSED SALT DATA (cond't)

Test No.	Electrolyte F=Fused S=Solution	Time (Min)	Current (amps)	Immersion Depth (Inch)	Area (In^2)	Current Density ($Amps/In^2$)
34	$NaNO_2$(F)	0.5	3.20	0.82	0.154	20.8
35	$NaNO_2$(F)	2.0	3.50	0.83	0.156	22.4
36	$NaNO_2$(F)	4.0	2.37	1.10	0.206	11.5
37	$NaNO_2$(S)	1.0	1.00	0.91	0.171	5.85
38	$NaNO_2$(S)	3.0	1.00	0.80	0.150	6.67
39	NaOH (S)	1.0	2.55	1.10	0.206	12.4
40	NaOH (S)	3.0	2.40	1.08	0.203	11.8

FUSED SALT DATA

Test No.	Weight Loss (grams)	Weight Loss Per Unit Length (grams/inch)	Comments
1	0.1317	0.244	Black Deposit on Cathode
2	0.0686	0.116	
3			
4	0.1548	0.352	
5	0.0141		
6	0.0599	0.103	Large Craters on Anode Surface
7	0.0727	0.117	
8	0.0237	0.0325	
9	0.0163	0.0220	
10			
11	0.0146	0.0228	Heavy ZN Plating on Cathode
12	0.0015	0.0230	
13	0.0154	0.0188	
14	0.0006	0.000790	
15	0.0002	0.00025	
16	0.0009	0.00097	
17	0.0010	0.00102	

FUSED SALT DATA (cond't)

Test No.	Weight Loss (grams)	Weight Loss Per Unit Length (grams/inch)	Comments
18	0.0009	0.00108	
19	0.0017	0.00189	
20	0.0298	0.0324	
21	0.2111	0.310	
22	0.0727	0.112	
23	0.2443	0.415	
24	0.0332	0.0510	
25	0.0219	0.0342	
26	0.0101	0.0131	
27	0.0366	0.0502	
28	0.0637	0.0545	High Convective Fluid Currents Observed in Electrolyte
29	0.1086	0.09[illegible]5	
30	0.1353	0.1353	
31	0.2357	0.2357	
32			
33	0.389	0.4474	
34	0.0409	0.0339	Current would peak & fall 10% in first minute (then level)
35	0.0169	0.0389	
36	0.0245	0.0270	
37	0.0121	0.0110	White Crystals Formed

FUSED SALT DATA (cond't)

Test No.	Weight Loss (grams)	Weight Loss Per Unit Length (grams/inch)	Comments
38	0.0412	0.0329	
39	0.0220	0.0242	Bubbles at both electrodes
40	0.0396	0.0428	

APPENDIX II HOLE DRILLING DATA

TESTS IN PRESSURE CHAMBER

Test No.	Tool No.	Tool Pres. psi.	Chmb Pres. psi.	Chmb Fluc. psi.	Max Feed "/min	Max Amps	Volts	Flow	C_c	Comments
2p	1-2		2000		.098	15	20			Shorted at .157 feed. Wide craterlike hole
3p	3-7	3000	2000		.118	10	20			Shorted at .218. Wide tapered hole.
4p	3-7	3000	2000		.334	40	40			Fairly uniform hole. No shorts. No tool wear.
5p	4-7	2800	2500	100	.433	20	40			Good hole, no shorts, no tool wear.
6p	4-7		2400		.71	40	40			Good hole, no shorts, no tool wear.
7p	4-7	2800	2600	100	.334	28	40	70	.043	No shorts, much higher feed possible. Wide shallow hole.
8p	5-7	2500	2400	50	.334	48	40	97	.055	No shorts, no tool wear. Good hole.
9p	5-7	2000	2000	100	.55	90	60	97	.18	Some arcing, clean, uniform diameter hole.
10p	5-7	2000	2000	200	.55	250?	80	195	.30	Lost insulation at tip. No arcing. Shallow wide hole.
11p	7-7	2600	2400	100	.71	150	36	65	.27	No arcing. Cut excellent hole. (See photo under testing)
12p	7-7		2200	50	.334	90	40	80	.13	Shorted at .90 feed. Shallow wide hole.
13p	7-7		2200	200	.55	95	40	80	.13	Shorted at .71 feed. Found table fluct. due Δp = cause.
14p	4-7	2900	1800	200	.079	100	40			Tungsten carbide work. Continuous arcing. High tool wear.
15p	7-8		2000	150	.55	65	40	130	.06	Cut deep somewhat irregular hole.
16p	4-7	2000	0	0	.218	14	40	130	.018	Continuous arc at .334 feed. OK at .218 feed.
17p	4-7	2700	1000	200	.55	45	40	115	.05	Very clean accurate tight hole.
18p	4-7	1750	500	50	.55	32	40	130	.05	Very smooth test. Limit--one small arc. Very deep narrow hole.

Test No.	Tool No.	Tool Pres. psi.	Chmb Pres. psi.	Chmb Fluc. psi.	Max Feed "/min	Max Amps	Volts	Flow	C_c	Comments
19p	4-7	1300	500	25	.218	14	40	130	.018	Continuous arc at .334 feed. OK at .218 feed.
20p	4-7	2900	2200	50	.71	45	40	130	.038	Very clean accurate tight hole.
21p	4-7		2000		.55	55	40	130	.049	Arcing then shorted. Insulation failure.
22p	4a-7	1700	0	0	.334	70	40	130	.3	Arc @ .079 at surface. Pressure in hole, ins. failed. rough hole N.G.
23p	4a-7	800	0	0	.118	300	40	130		Strong continuous arcing.
24p	4a-7	2300	1000	100	.55	45	40	130	.05	Occasional Arc. Good deep narrow hole.
25p	4a-7	1700	500		.433	75	40	130	.10	Heavy arcing at .55 feed. Irregular rough hole.
26p	4a-7	2500	1500	150	.55	100+	40	130	.10	Short -- insulation failure. Cavity type hole.

Testing dates: 2p--4p, 4-21-66 / 5p--7p, 4-27-66 / 8p--10p, 4-28-66 / 11p--13p, 5-4-66 / 14p--15p, 5-6-66 / 16p--17p, 5-9-66 / 18p-21p, 5-10-66 / 22p--26p, 5-12-66.

C_c was calculated from eq. 2.5, $T_o = 100^{\circ}F$, T_b from stream tables.

Flow rates given in $in.^3/min$.

All maximum feed rates given are for tool at least 3/8" into the workpiece.

Entry feed rates are only shown on graph of max. feed versus pressure.

HOLE DRILLING DATA

Workpiece Material: Steel (1080)
Tool: 4-7a
Voltage Configuration: D.C.
Electrolyte: NaCl Solution

Test No.	Electrolyte Composition % (Weight)	Tool Pressure (psi)	Chamber Pressure (psi)	Flow Rate (at max feed) (in^3/min)	Entry Feed Rate (in/min)	Max. Feed Rate (in/min)	Tool Diameter (in)
31-P	11	2500	2000	72.6	.218	.334	.091
32-P	11	2800	2000	84	.218	.334	.083
33-P	11	2900	2500	75	.218	.55	.080
34-P	11	2800	2300	64	.275	.71	.079
35-P	11	3000	2500	58	.218	.90	.086
36-P	20	2700	2200	78	.218	1.18	.087
37-P	20	2500	1000	24	.157	.334	- -
38-P	20	2800	2400	93	.218	.334	- -
39-P	20	2500	2200	23	.275	.275	- -
40-P	20	3000	2500	70	.275	.275	.084
75-P	20	3500	2400	36	.275	1.18	.080
76-P	20	3500	2200	68	.275	1.53	.082
77-P	20	3500	2000	97	.230	1.42	.075
78-P	20	3500	2400	97	.230	1.42	.077

HOLE DRILLING DATA

1080 Steel (cond't)

Test No.	Voltage	Max. Current (Amps)	Hole Area @ Max. Feed (in^2)	Max. Current Density ($amps/in^2$)	Tool	Comments: Hole	Comments: Test
31-p	80	16.	.00679	2360	Insl. Good	1/4" Deep	--
32-p	80	25	.00785	3190	Bent	Uniform Diam.	--
33-p	80	38	.00567	6700	No Insl. Loss	Uniform Diam.	Complete
34-p	80	65	.00950	6840	Good	- -	Complete
35-p	80	58	.00679	8550	Good	Good Finish	Complete
36-p	80	120	.0112	107	Good	- -	Failed
37-p	20	10 (short)	.158	64	Lost 3/4" Insl.	- -	Failed
38-P	20	10 (short)	-	-	Tip damage	1/8" Deep	Failed
39-p	120	20 (short)	-	-	Bent	Crater	Failed
40-p	40	70	.254	275	Slight Insl. Loss	1/2" Deep	A.C. Failed
75-p	80	175	-	-	Insl. Loss	Crater	High Feed Rate
76-p	80	85	.00635	13400	Tip Damage	Crater @ Top	Complete
77-p	80	125	.00635	19700	No Wear	Good Hole	Complete
78-p	80	90	.00515	17500	No Wear	Good Hole	Complete

HOLE DRILLING DATA

Workpiece Material: Tungsten Carbide
Tool: 4-7a (Brass)

Test No.	Tool Pressure (psi)	Chamber Pressure (psi)	Flow Rate at Max Feed (in^3/min)	Max Feed Rate (in/min)	Electrolyte (20% by weight)
41	2800	2000	70	.079	NaCl
42	2800	2000	70	.118	NaCl
43	3000	2200	58	.079	NaCl
44	3000	1500	58	.079	NaCl
45	3000	2000	46	.118	NaCl
46	2600	2000	46	.098	NaCl
47	2500	2000	70	.098	NaCl
48	2800	2600	70	.079	NaCl
49	3000	2000	70	.079	NaCl
50	2600	2200	70	.079	NaCl
51	2800	2000	93	.079	NaCl
60	2800	2500	70	.079	NaOH
61	2700	2500	70	.079	NaOH
62	3000	2600	47	.079	NaOH
63	2600	2400	70	.079	NaOH
64	2800	2600	70	.079	NaOH
65	3000	2400	47	.079	NaOH
66	3000	2800	47	.098	NaOH
67	2800	2600	47	.098	NaOH
68	2800	2600	47	.098	NaOH
69	3000	2800	23	.098	NaOH
79	--	--	47	.098	NaOH

HOLE DRILLING DATA

Tungsten Carbide (continued)

Test No.	Voltage Frequency (cps)	Duty Cycle (on : off)	Wave Type
41	55	8:1	Pos. DC Square Wave
42	55	8:1	Same as #41
43	22	22:1	Pos. DC Sq. Wave H.V. Pulses
44	50	8:1	Same as #43
45	50	8:1	Same as #43
46	50	8:1	Same as #43
47	50	8:1	Pos. DC Sq. Wave
48	50	8:1	Pos. DC Sq. Wave
49	83	5:1	Pos. DC Sq. Wave
50	1000	2:1	Pos. DC Sq. Wave
51	1000	2:1	Same as #50
60	750	2:1	Pos. DC Sq. Wave
61	1000	2:1	Same as #60
62	1000	2:1	Same as #60
63	750	2:1	Pos. DC Sq. Wave
64	750	2:1	Same as #63
65	750	2:1	Same as #63
66	1000	2:1	Pos. DC Sq. Wave
67	1000	2:1	Same as #66
68	1000	2:1	Same as #66
69	2000	1:1	Pos. DC Sq. Wave
79	1000	1:1	Pos. DC Sq. Wave

HOLE DRILLING DATA

Tungsten Carbide (continued)

Test No.	Average Tool Voltage (volts)	Average Tool Current (amps)	Tool Diameter (in)	Hole Area (In^2)	Current Density ($amps/in^2$)
41	40	8	.084	.00515	1550
42	60	13	.085	.00635	2050
43	40	15	.087	.00679	2150
44	40	13	.091	--	--
45	80	--	--	--	--
46	80	--	.086	--	--
47	80	20	.081	--	--
48	40	17	.142	--	--
49	40	10	.083	.00568	1760
50	40	6	.084	.00679	884
51	40	--	.081	--	--
60	40	6	.085	.00515	1070
61	36	8	.086	.00850	940
62	32	17	.085	--	--
63	31	18	.080	.00694	2600
64	--	--	.085	.00635	--
65	--	--	.088	.00785	--
66	34	12	.082	.00635	1890
67	40	--	.081	--	--
68	34	12	.080	.00635	1890
69	40	--	.083	--	--
79	40	--	.085	--	--

HOLE DRILLING DATA

Tungsten Carbide (continued)

Test No.	Tool	Comments Hole	Test
41	Tip & Insl. Damaged	Thru w-c chip (rough)	Much arcing
42	Tip & Insl. Damaged	Tapered Hole	Arcing problems
43	Tip & Insl. Damaged	Rough Hole	Arcing + Poor Press. Reg.
44	Insl. Damage	Beginning of Hole	Failure
45	Tool Melted	Crater	Failure
46	Tip & Insl. Damaged	Crater	Failure
47	Tip Damage	Crater	Failure
48	Tip Damage Crater	Crater	Failure
49	No Damage	1/2 thru chip	Good (arcing)
50	Insl. Damage	0.9 thru chip	Good (arcing)
51	Bent	Nothing	Failure
60	Bent & Damaged	No Round, but thru	Good
61	Bent	Good Hole	Complete Test
62	Bent + Insl. Loss	- -	Failure
63	No Damage	Good Hole	Complete
64	Bent (No Wear)	Nothing	Failure
65	Bent	1/8" Penetration	Failure
66	Bent (No Wear)	1/4" Deep (Poor Finish)	Deepest Penetration
67	Lost 1/16 inch	Nothing	Failure
68	Slight Insl. Wear	1/8" Deep Good Hole	Good Test
69	No Wear	Nothing	Failure
79	No Wear	Nothing	Failure

HOLE DRILLING DATA

Material: Nickel Alloy (Ni 76.4, Cr 15.85, Cu 0.10, Fe 7.2, Mn 0.20, Si 0.20, C 0.40, S 0.007)

Voltage: 40 VDC, All Tests

Electrolyte: NaCl (20% by Weight)

Tool: 4-7a (Brass)

Test No.	Tool Pressure (psi)	Chamber Pressure (psi)	Flow Rate (in^3/min)	Entry Feed Rate (in/min)	Max Feed Rate (in/min)	Tool Diameter (in)
52	2800	2400	48.5	0.157	0.334	-
54	2700	2200	64.0	0.218	0.55	0.080
56	3000	2600	38.8	0.275	0.71	0.080
70	3500	3000	NaOH Electrolyte - Unsuccessful Attempt			
72	-	-	-	0.218	0.218	-
73	3500	3000	44.7	0.157	0.57	0.083
74	3800	3500	24.3	0.157	0.433	0.085

HOLE DRILLING DATA

Nickel Alloy (cond't)

Test No.	Max Current (amps)	Hole Area @ Max Feed	Max Current Density (amps/in^2)	Tool	Comments Hole	Test
52	40	0.0100	4000	1/4" Insl Loss	Large, Smooth	-
54	75	0.00568	13200	Slight Tip Wear	Deep	Erratic Current
56	52	0.00635	8200	No Wear	Deep + Tight	Complete
70	Test Failed					
72	-	-	-	Melted	Sloppy	Failure
73	30	-	-	No Wear	Crater	Failure
74	40	0.00568	7050	No Wear	Deep	Complete

HOLE DRILLING DATA

Material: Cobalt Alloy - Haynes Stellite (C 0.20, Cr 20.0, B 0.02, Ni 27.0, W. 12.0, Ta 2.0, Ti 3.8, Co balance)

Electrolyte: NaCl (20% by weight)

Tool: 4-7a (Brass)

Test No.	Tool Pressure (psi)	Chamber Pressure (psi)	Flow Rate (in^3/min)	Entry Feed Rate (in/min)	Max Feed Rate (in/min)	Tool Diameter (inch)
53	2800	2000	58.4	0.098	0.334	- -
55	2800	2200	48.6	0.157	0.433	0.073
57	2800	2200	46.8	0.218	0.433	- -
58	3000	2400	58.3	0.157	0.334	0.085
59	3000	2400	58.3	0.157	0.55	0.081
71	NaOH Electrolyte		Unsuccessful Attempt		--	- -

HOLE DRILLING DATA

Cobalt Alloy (cond't)

Test No.	Voltage	Max Current (Average for Pulsed) (amps)	Hole Area @ Max Feed (in^2)	Max Current Density ($amps/in^2$)	Comments		
					Tool	Hole	Test
53	40 V.D.C.	100	0.0167	- -	Insl. Loss	Crater	Poor
55	40 V.D.C.	35	0.0048	7400	Little Wear	Deep+Tight	Complete
57	40 V.D.C.	40	.00568	7050	Insl. Loss	Sloppy	Complete
58	Pulsed*	38	.00515	7340	Insl. Loss	Shallow	Shorted
59	Pulsed	58	.00568	10200	No Wear	Good Hole	Complete
71	Test Failed						

*Pulsed D.C. 750 cps.

2:1 on:off Ratio

Transient Voltages Provided Neg. Pulse Effect

APPENDIX III

The Laser

The E.C.M. laser experiments were performed using single pulses of high intensity light from a ruby laser. This laser was constructed in the Materials Processing Laboratory at M.I.T., and the following is a description of the apparatus and its operation. Further information may be obtained from the references at the end of this appendix.

Figure A-3-a shows the ruby rod and flash tube configuration along with a circuit diagram. The rod is a single crystal of Al_2O_3 with approximately .05% chromium. One end is 99.1% reflective, while the other end is only 80% reflective. It is surrounded by six FX-100 xenon flash lamps which are in turn surrounded by an aluminum reflector. The flash lamps are connected in series, and are used as a pump source for the ruby rod.

The 5 K.V. supply is used to charge the 5 mfd capacitor through R_1. The flash tubes are then triggered by a 30 K.V. pulse. The Inductor I is placed in the circuit to limit the rate of discharge of the capacitor through the flash tubes (I is 100 turns of #16 wire on a 2" D. core). R_2 and S_1 are placed in the circuit as a safety feature, as they allow any charge remaining on the capacitor to be drained off after the laser has been fired.

The laser beam is focused through a one inch focal length microscope objective. This is accomplished by removing the ruby rod, shining a flashlight through the apparatus, and focusing. Once this is done, the ruby rod is replaced, the capacitor charged, and the 30 K.V. supply triggered, thus giving a high intensity pulse of laser light. Between firings, the ruby rod is removed and cooled in alcohol.

APPENDIX IV

TOOL DATA:

Tool No.	Material	Type*	A	B	C	D	E	F
1	Stainless	AA	.100	.80	.60	1 5/8	-	-
2	Aluminum	DD	.100	.100	1/16	1 3/4	-	-
3-7	Brass	BB	.085	1/16	1/32	1 1/2	-	-
4-7	Brass	CC	.085	1/16	1/32	1 1/2	1/2	.125
4a-7	Brass	CC	.085	1/16	1/32	1 3/4	1/2	.125
5-7	Stainless	DD	.122	.100	1/16	1 5/8	-	-
6-7	Stainless	EE	.122	.100	1/16	1 7/8	1/4	.150
7-7	Brass	BB	.145	.125	1/16	1 3/4	-	-
4-8	Brass	CC	.090	1/16	1/32	1 1/2	1/2	.125
7-8	Brass	BB	.140	.125	1/16	1 3/4	-	-

* Type -- see drawings of tool geometries page 26 & 27.
All dimensions are given in inches.

TOOL NUMBERING SYSTEM:

Example 4-7

The number before the dash gives the metal part of the tool -- the geometry or Type and all dimensions except for A. It also given the material (brass, aluminum, stainless, etc.)

The number after the dash gives the insulation type. These numbers are explained in the section on Development of the Tool and Insulation.

The general tool number, 4-7 for example, completely specifies the tool -- material, dimensions and insulation.

TEST RUN NUMBERING SYSTEM:

The tests are simply numbered in a chronological manner, one number per test. A p is added to the number if the test is run in the pressure chamber. The number alone is suggicient to specify the test -- the p is simply additional information.

SAMPLE NUMBERING SYSTEM:

The samples are numbered chronologically with a b added if it is set in bakelite.

APPENDIX V

PROCEDURE FOR RUNNING A TEST:

I. Electrolyte Supply

A. Set low pressure flow valves in proper position.
B. Set electrolyte return valves to return fluid to tank.
C. Pressurize accumulator with nitrogen to 2000 psi.
D. Make sure tool throttling valve is closed.
E. Start low pressur pump.
F. Start high pressure pump.

II. Mechanical setup -- Plexiglas tank

A. Clamp workpiece in place.
B. Put tool in tool holder.
C. Screw down tank cover.
D. Feed Tool down to desired clearance over workpiece.

III. Machining Test -- Plexiglas tank

A. Set desired electrolyte flow with tool throttling valve. Start exhaust blower.
B. Set power supply at desired voltage.
C. Engage feed clutch with feed selector at desired entering feed.
D. For feed changes disengaged feed clutch, change feed, reengage feed clutch.
E. To stop test reverse feed, then turn off power supply, then turn off electrolyte flow.

IV. Mechanical set-up -- Pressure Chamber

A. Clamp bakelite-mounted specimen in place making sure that all surfaces are dry and that base and upper o-rings are in place.
B. Check that tank base to contact electrode resistance is above 10^6 ohm. (Seals dry)
C. Check that specimen is in contact with contact electrode.
D. Make measurements on scale for contact position and maximum depth of hole position.
E. Put on chamber head and feed tool down to desired tool - work clearance.

V. Machining Test -- Pressure Chamber

A. Open tool throttling valve and flush chamber for a short time.
B. Regulate flow rate and chamber pressure by use of the two throttling valves and pressure regulator.
C. Set power supply to desired voltage making sure that only slight current is drawn with tool - work clearance. (Checks for bad insulation seals)
D. Engage feed clutch.
E. Change feed rates by declutching, changing, re-engaging clutch.
F. To stop test in case of emergency -- unusually high current -- immediately shut off power first, reverse feed, shut down electrolyte flow. Immediate shutting down of power helps to save contact electrode, seals, and base from severe arcing damage.
G. To stop test at end of run shut off feed, then power, and last electrolyte flow.

VI. Shutting down equipment and flushing system.

A. Close valves to tank.
B. Set return valves to drain.
C. Turn on fresh water supply.
D. Let water run through machining area and also backwards through low pressure pump and filter.
E. Pressurize and Depressurize accumulator at least five times to flush out electrolyte.
F. In general make sure that fresh water has flowed through all paths taken by the electrolyte.
G. Shut down water supply and close all drain lines.
H. Wipe and oil milling machine and make sure that all power to pumps, power supply, recording equipment, etc. is shut off.

VI. ILLUSTRATIONS

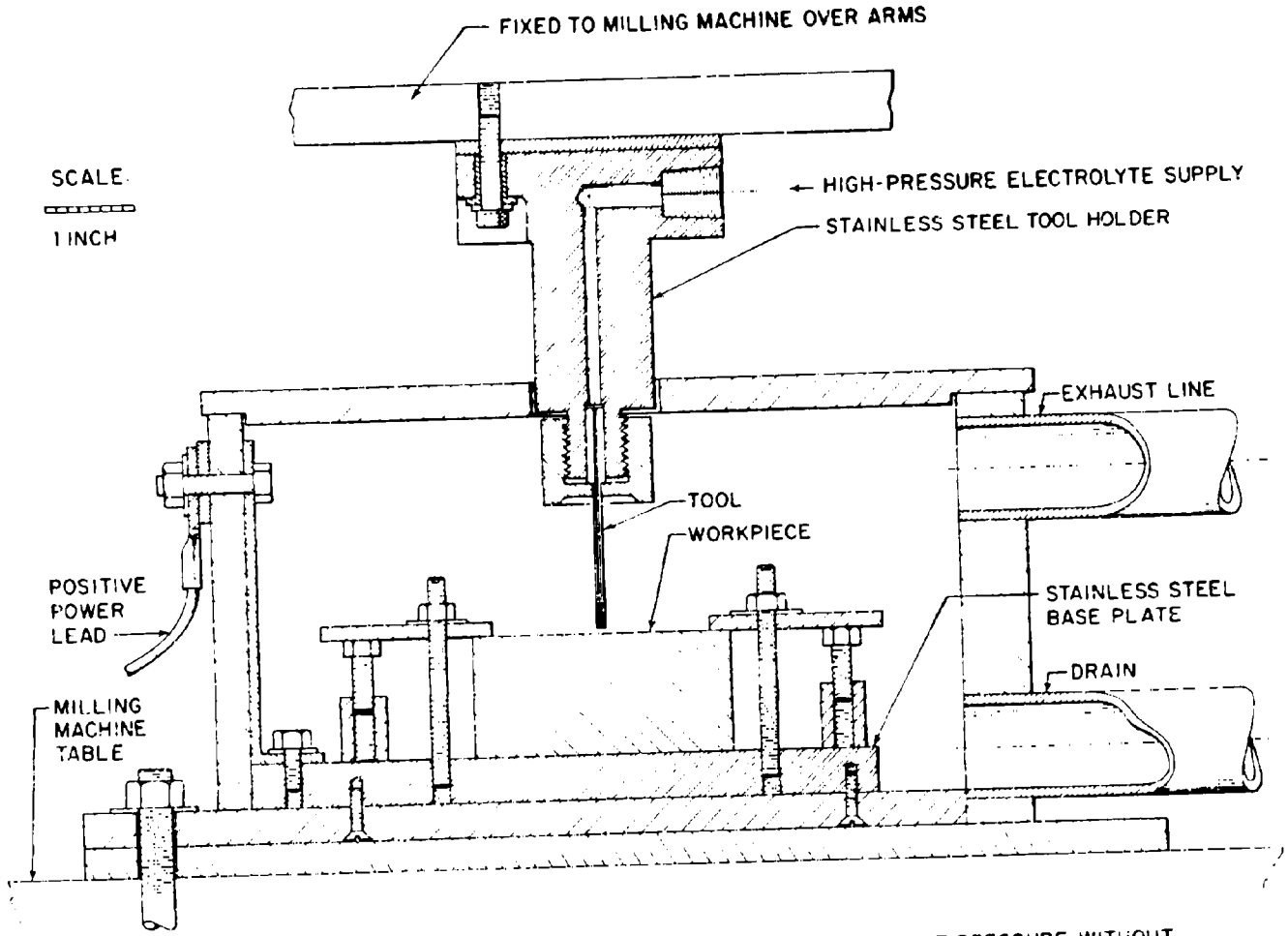

Fig. 2-1 ELECTRO-CHEMICAL MACHINE TOOLING FOR MACHINING AT ATMOSPHERIC EXIT PRESSURE WITHOUT PRESSURE CHAMBER

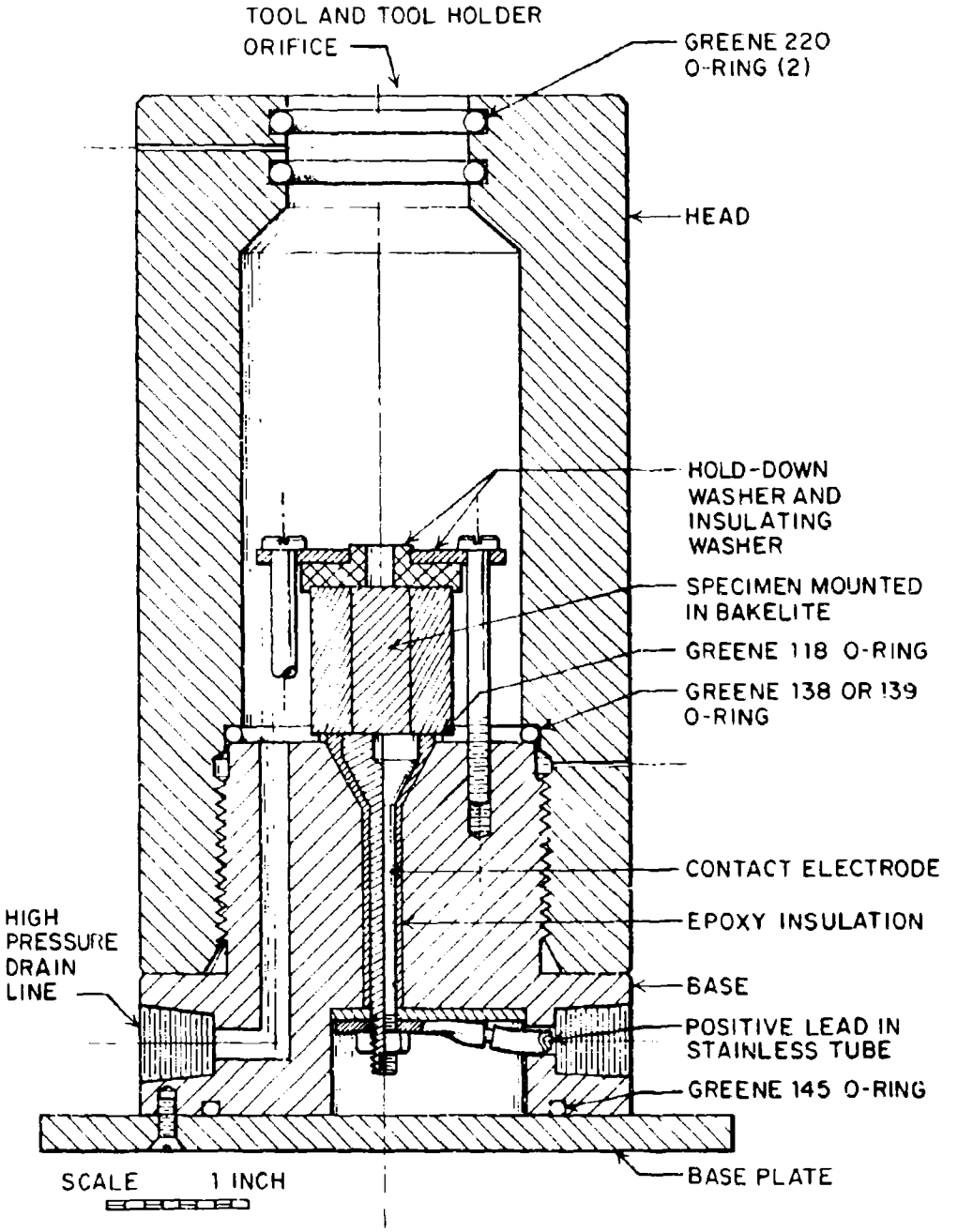

Fig. 2-2 E.C.M PRESSURE CHAMBER

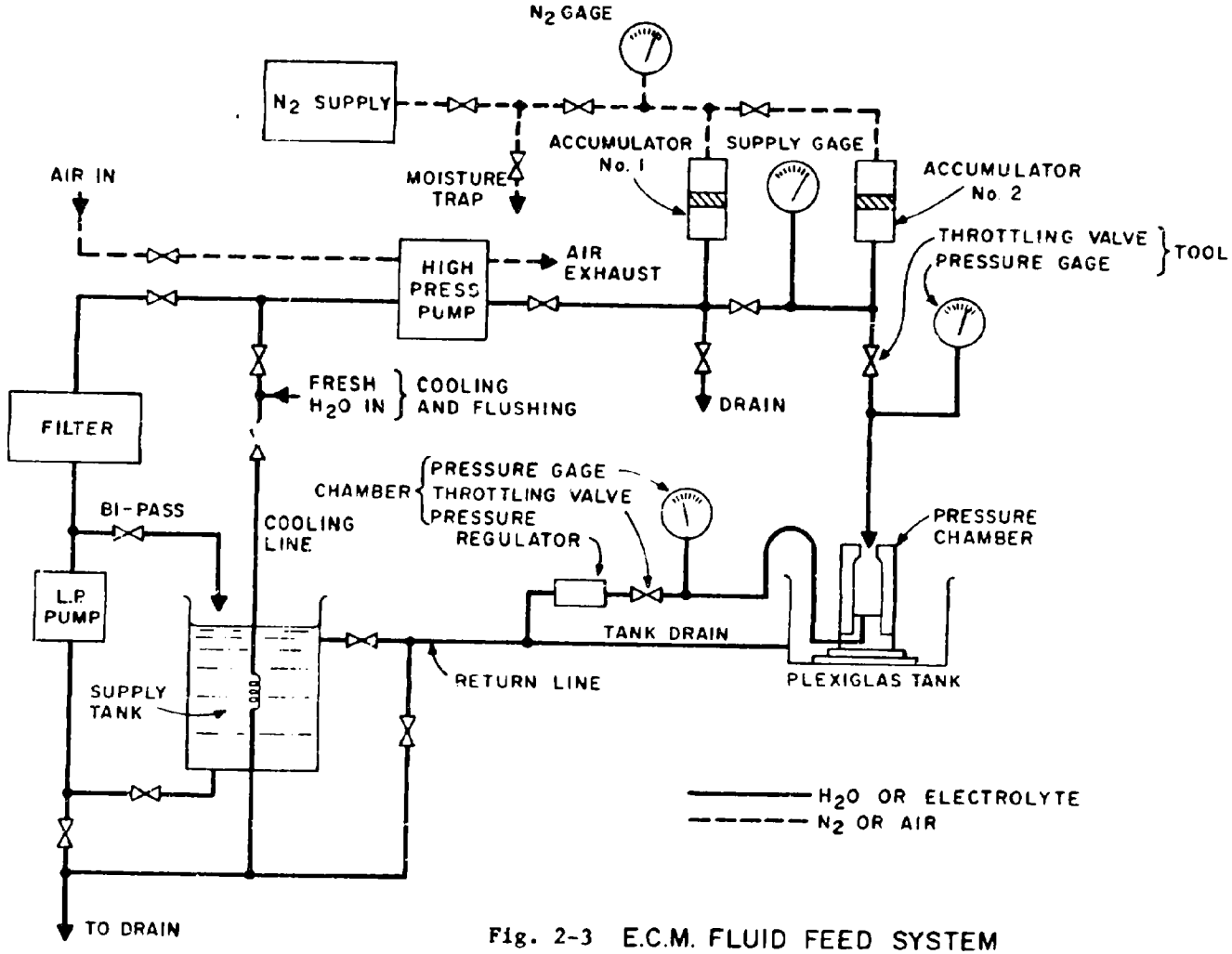

Fig. 2-3 E.C.M. FLUID FEED SYSTEM

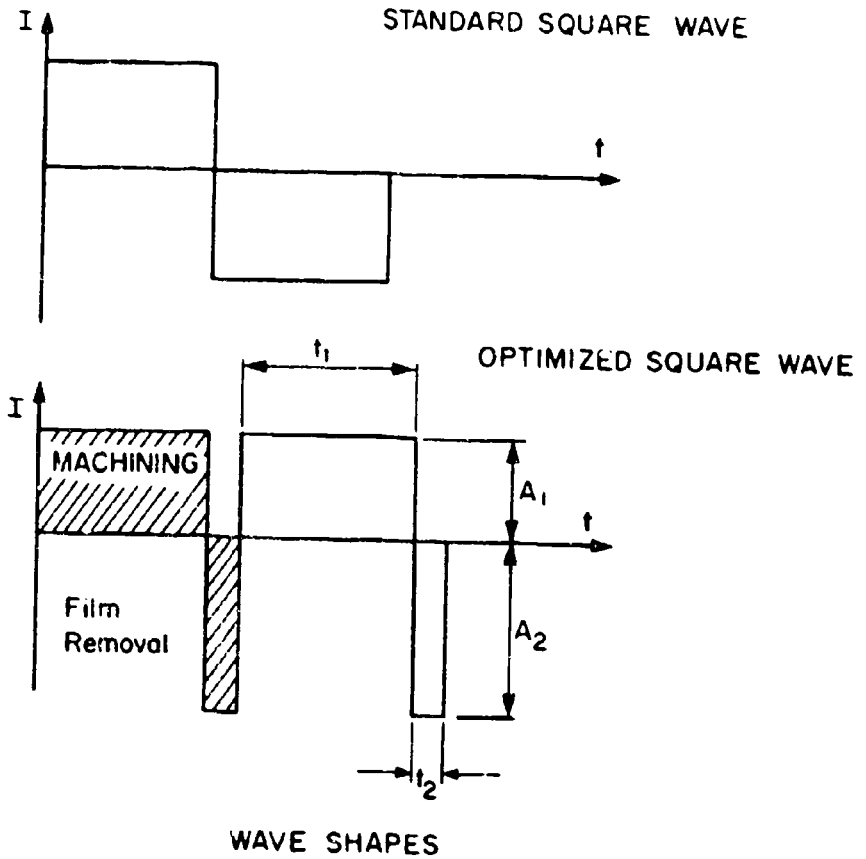
I
STANDARD SQUARE WAVE
t
t_1
OPTIMIZED SQUARE WAVE
I
MACHINING
A_1
t
Film
Removal
A_2
t_2
WAVE SHAPES

Fig. 2-4

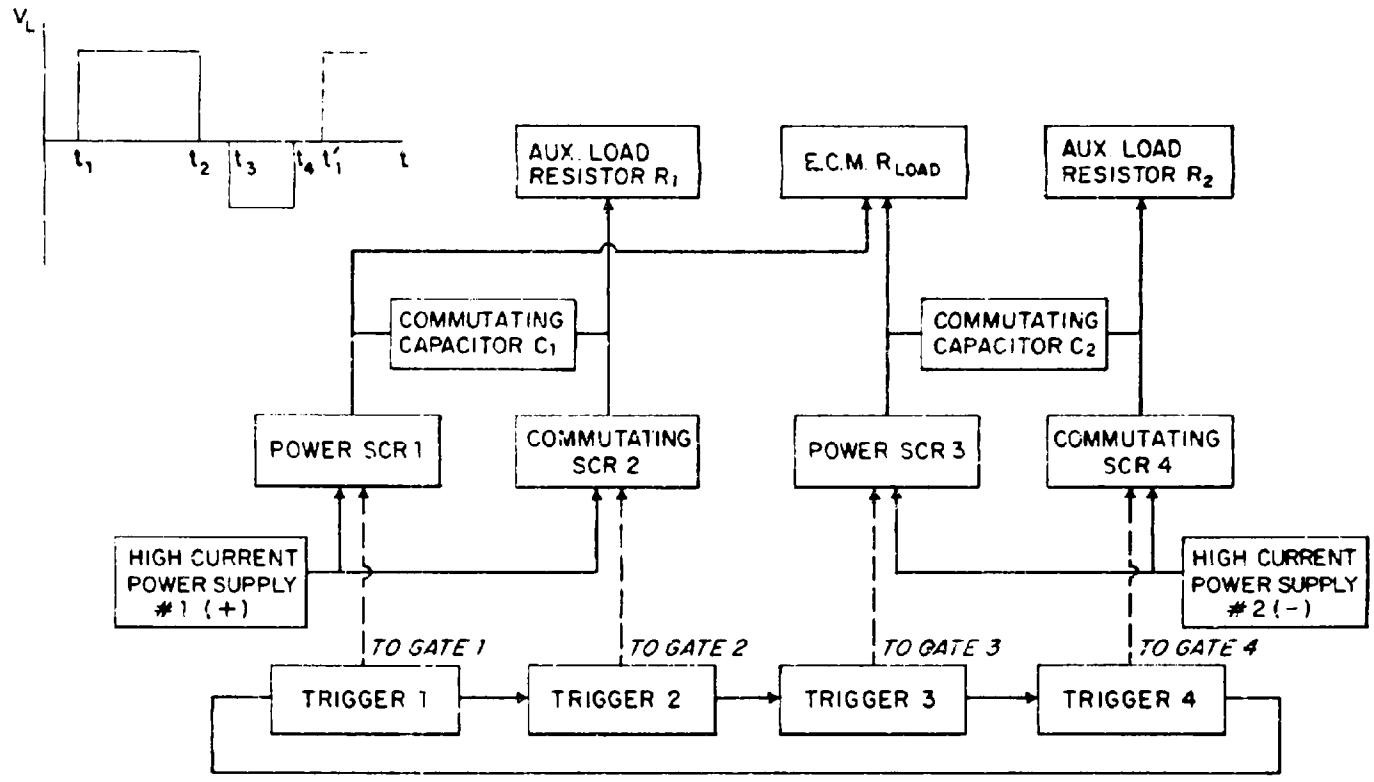

Fig. 2-5 BLOCK DIAGRAM E.C.M. POWER SUPPLY

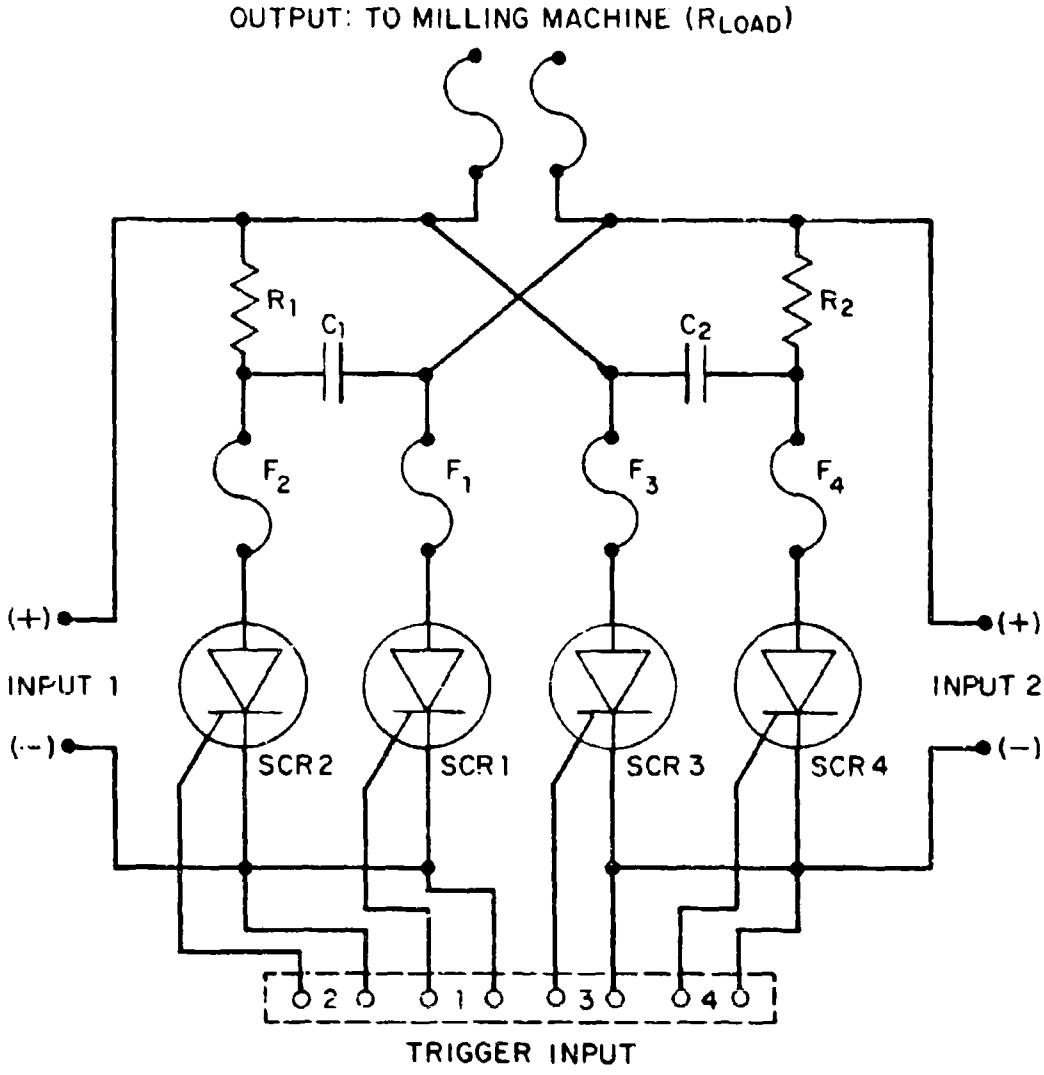

Fig. 2-6 100 AMP SWITCH - SCR 1,2,3,4 - 2N2027
R_1, R_2 = 1Ω - C_1, C_2 = $28/R_L \mu f$ - $F_{1,2,3,4,5,6}$ (AMP TRAP FORM 101)

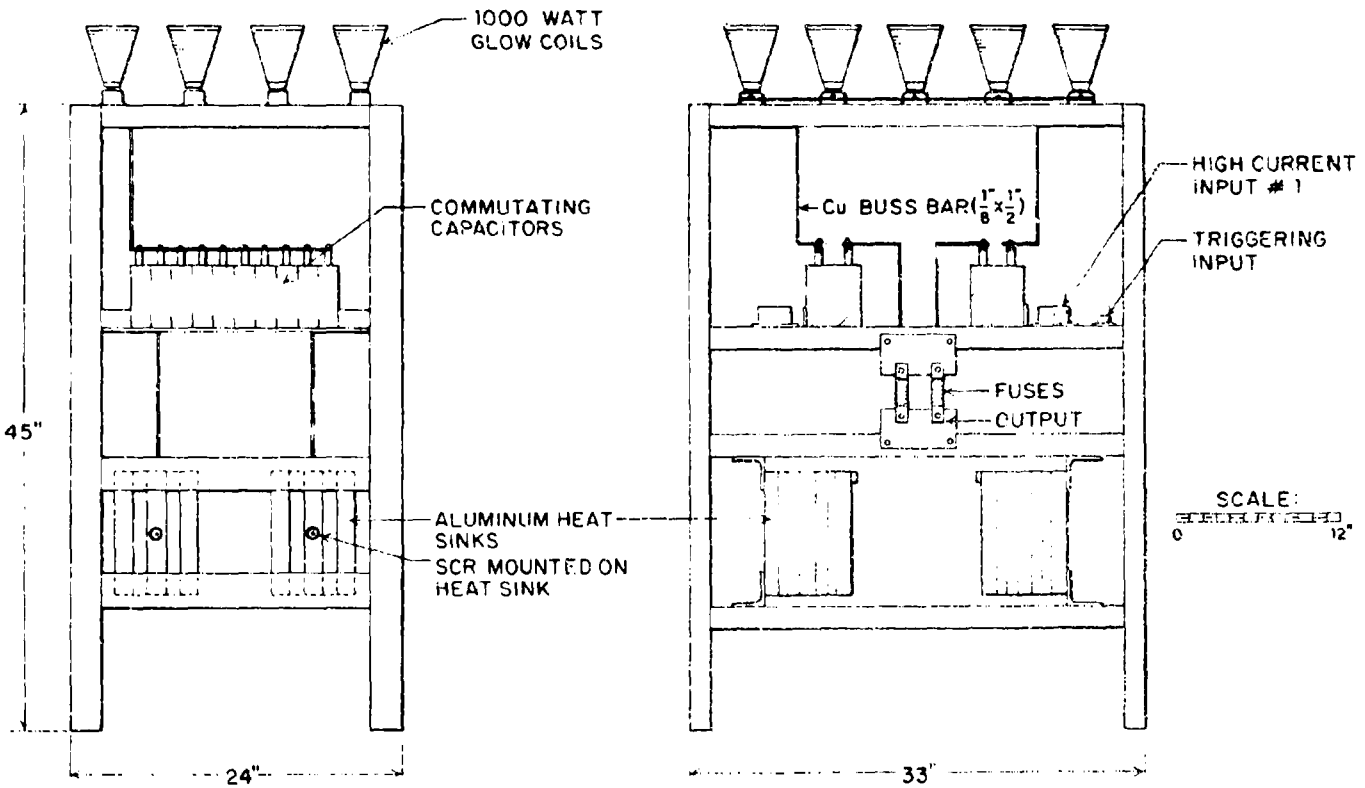

Fig. 2-7 HIGH CURRENT COMPONENTS. MATERIAL: $1\frac{1}{2}$"x$2\frac{1}{4}$" STEEL ANGLE

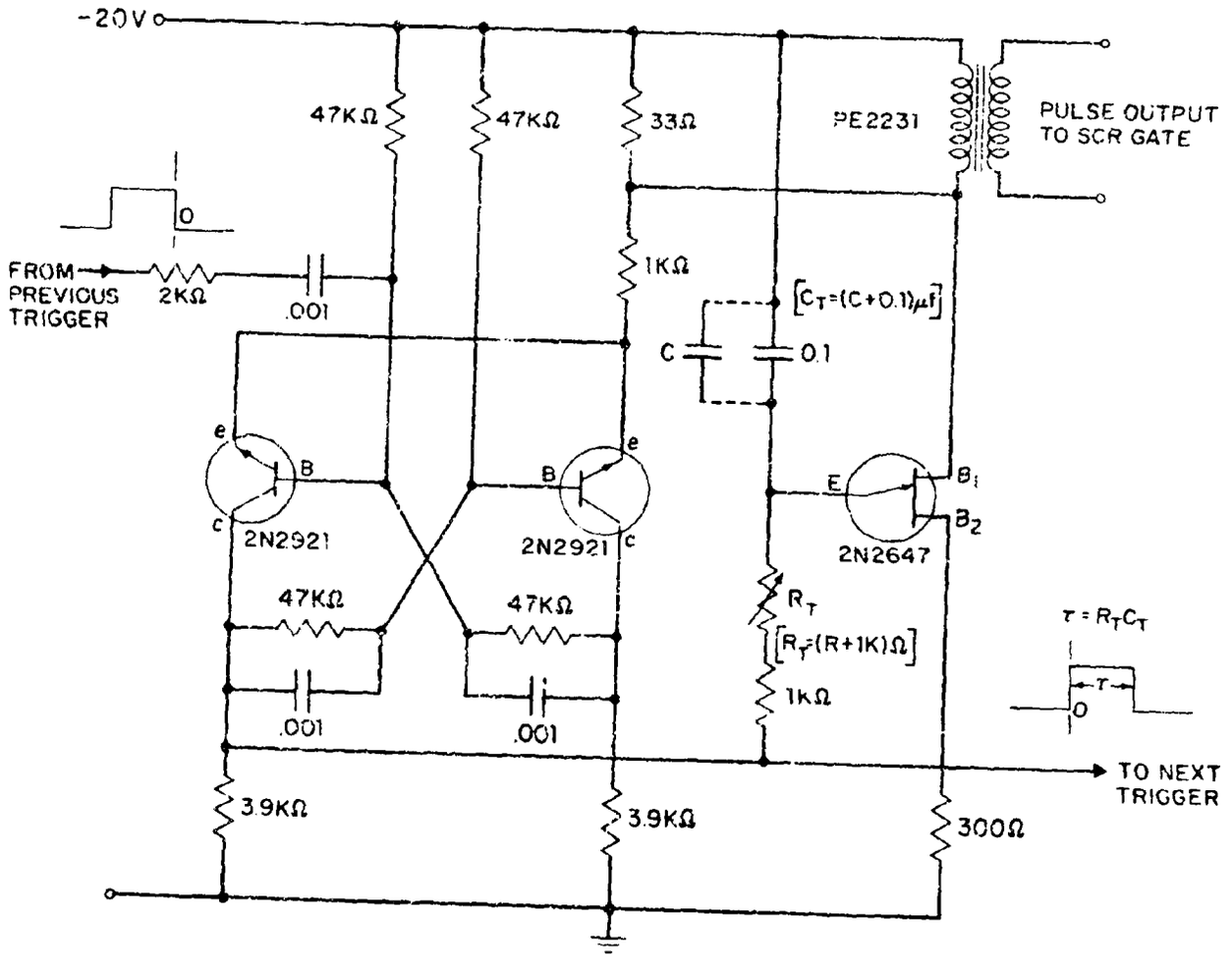

Fig. 2-8 TRIGGER CIRCUIT

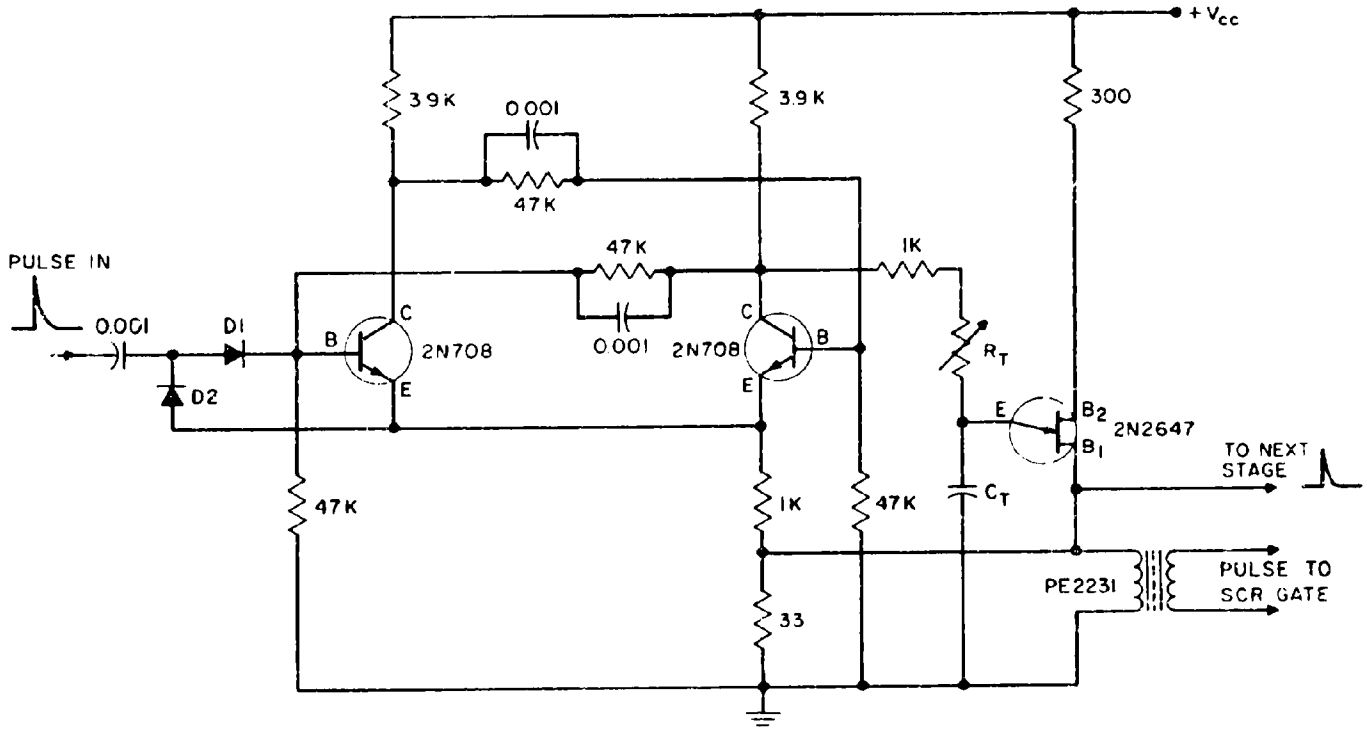

Fig. 2-9 REVISED TRIGGER CIRCUIT

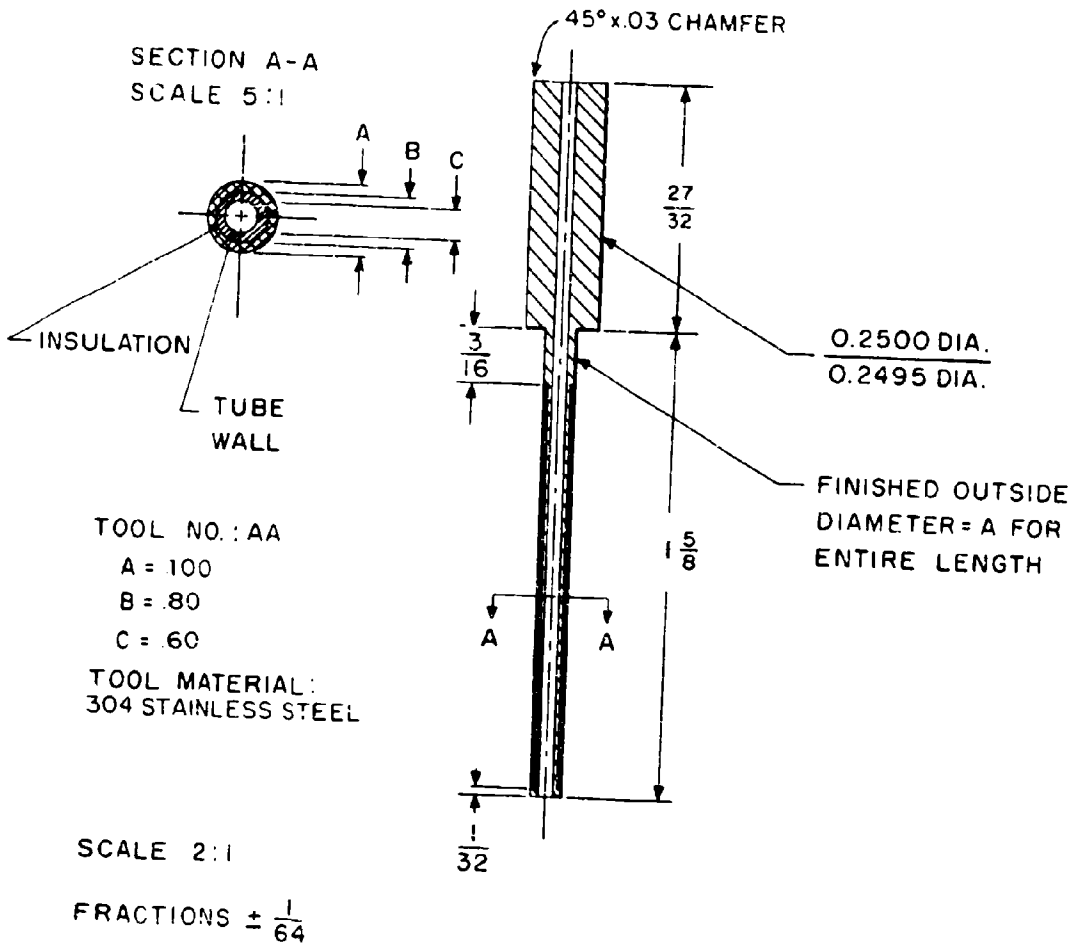

Fig. 2-10 ELECTRO TOOL AA

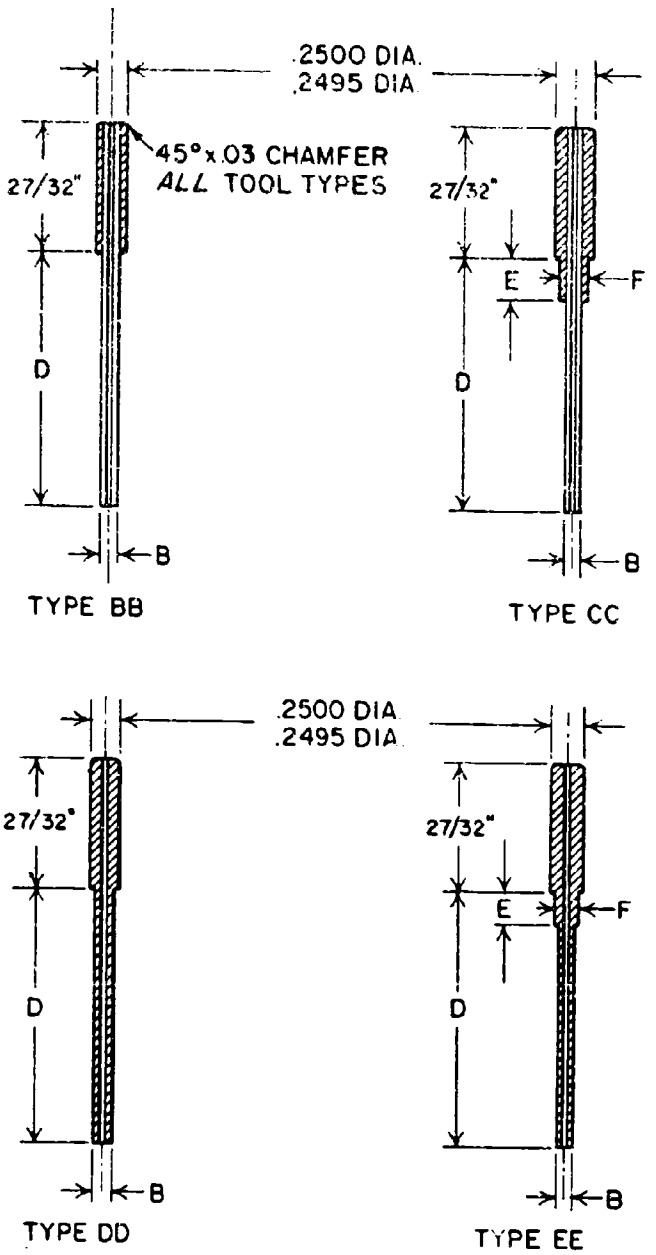

BORE DIAMETER = DIA. C
B DIA. + INSULATION = DIA. A

Fig. 2-11 TOOL TYPES

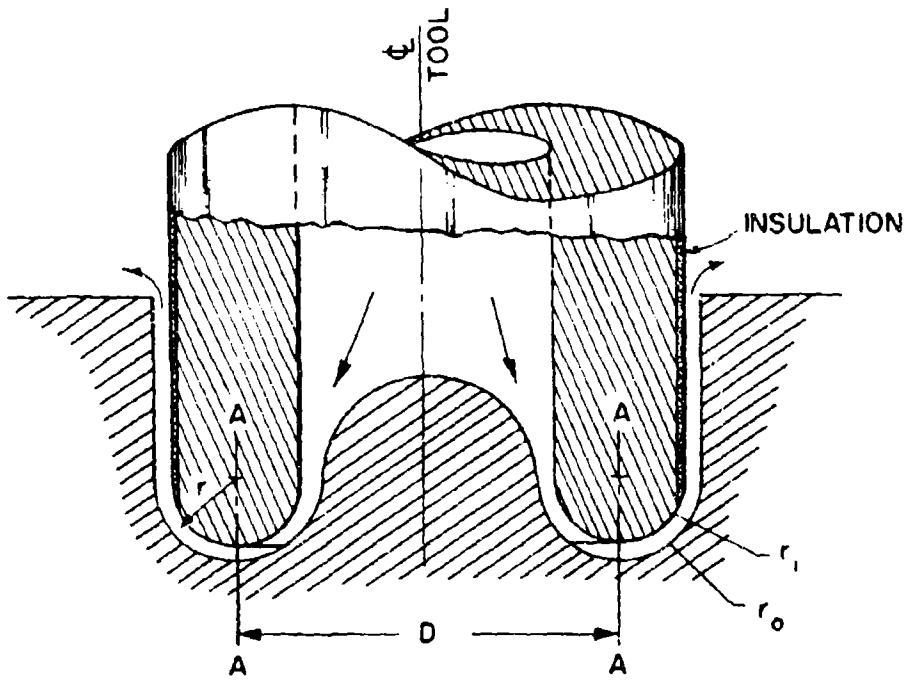

Fig. 3-1 ASSUMED TOOL-WORK GEOMETRY

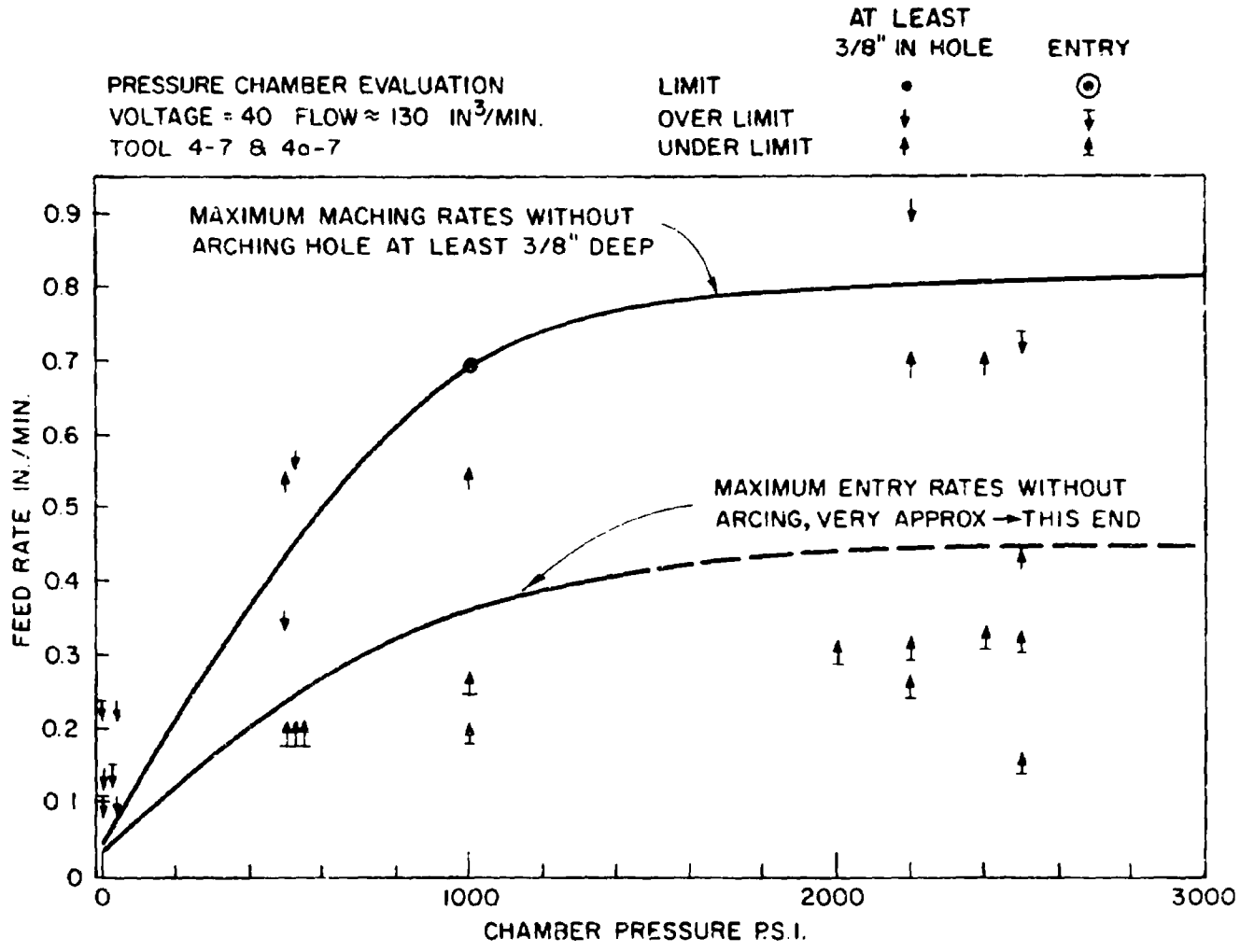
AT LEAST
3/8" IN HOLE
ENTRY
PRESSURE CHAMBER EVALUATION
VOLTAGE = 40 FLOW ≈ 130 IN³/MIN.
TOOL 4-7 & 4a-7
LIMIT
OVER LIMIT
UNDER LIMIT
MAXIMUM MACHING RATES WITHOUT
ARCHING HOLE AT LEAST 3/8" DEEP
MAXIMUM ENTRY RATES WITHOUT
ARCING, VERY APPROX →THIS END
FEED RATE IN./MIN.
0
0.1
0.2
0.3
0.4
0.5
0.6
0.7
0.8
0.9
0
1000
2000
3000
CHAMBER PRESSURE P.S.I.

Fig. 3-2

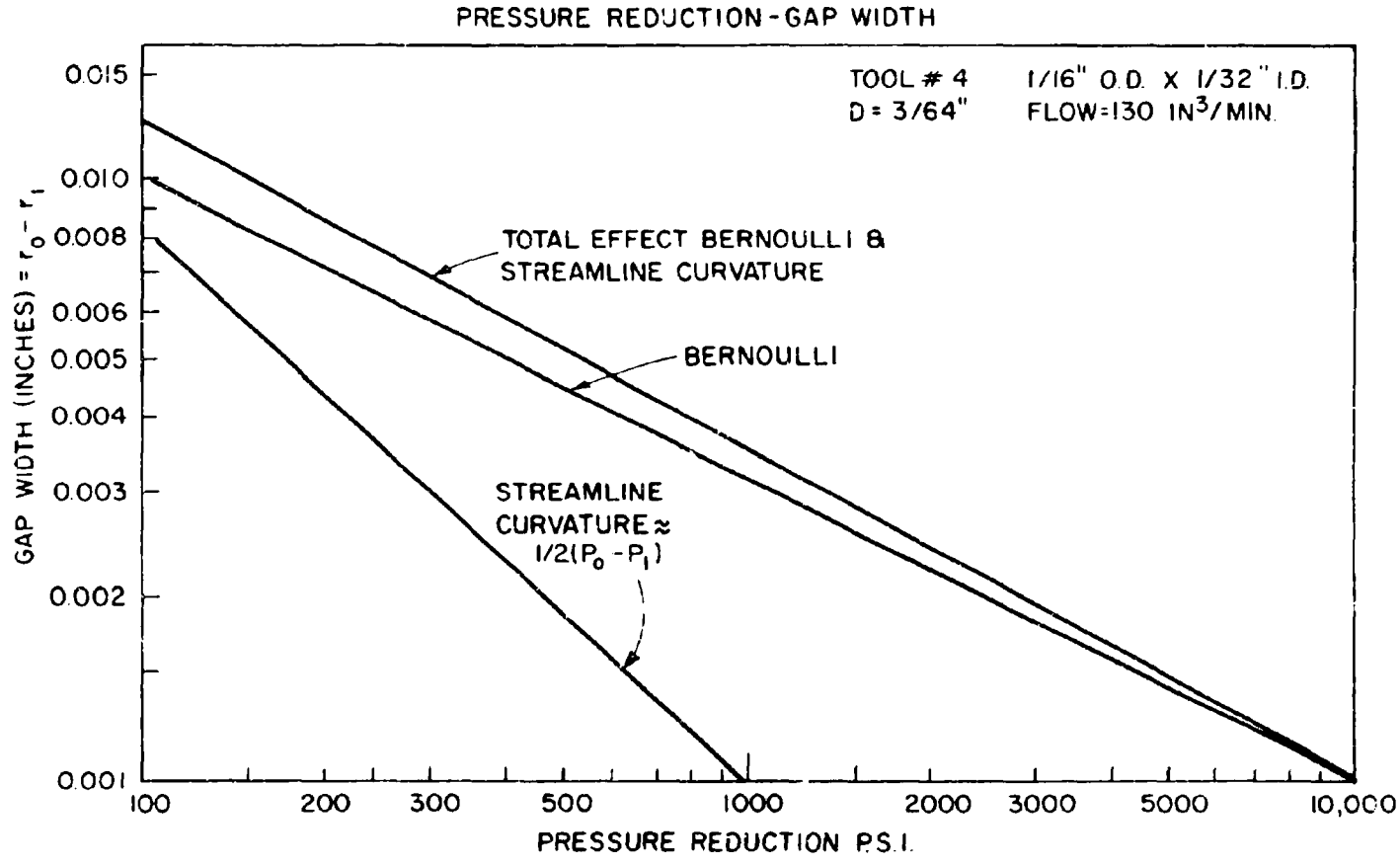
PRESSURE REDUCTION - GAP WIDTH
TOOL # 4
D = 3/64"
1/16" O.D. X 1/32" I.D.
FLOW=130 IN³/MIN.
TOTAL EFFECT BERNOULLI & STREAMLINE CURVATURE
BERNOULLI
STREAMLINE CURVATURE ≈ 1/2(P₀ - P₁)
GAP WIDTH (INCHES) = r₀ - r₁
0.015
0.010
0.008
0.006
0.005
0.004
0.003
0.002
0.001
100
200
300
500
1000
2000
3000
5000
10,000
PRESSURE REDUCTION P.S.I.

Fig. 3-3

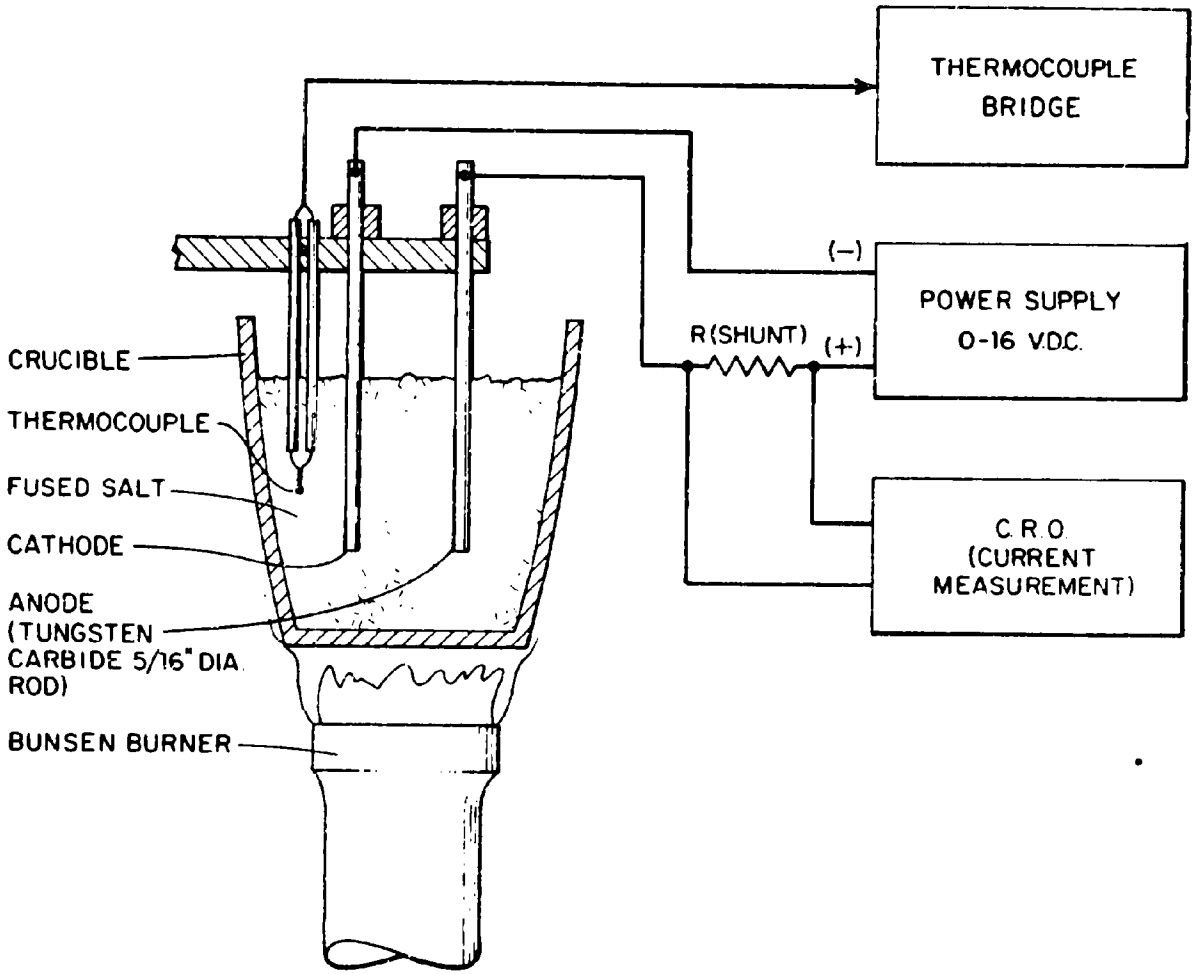

Fig. 4-1 FUSED SALT APPARATUS

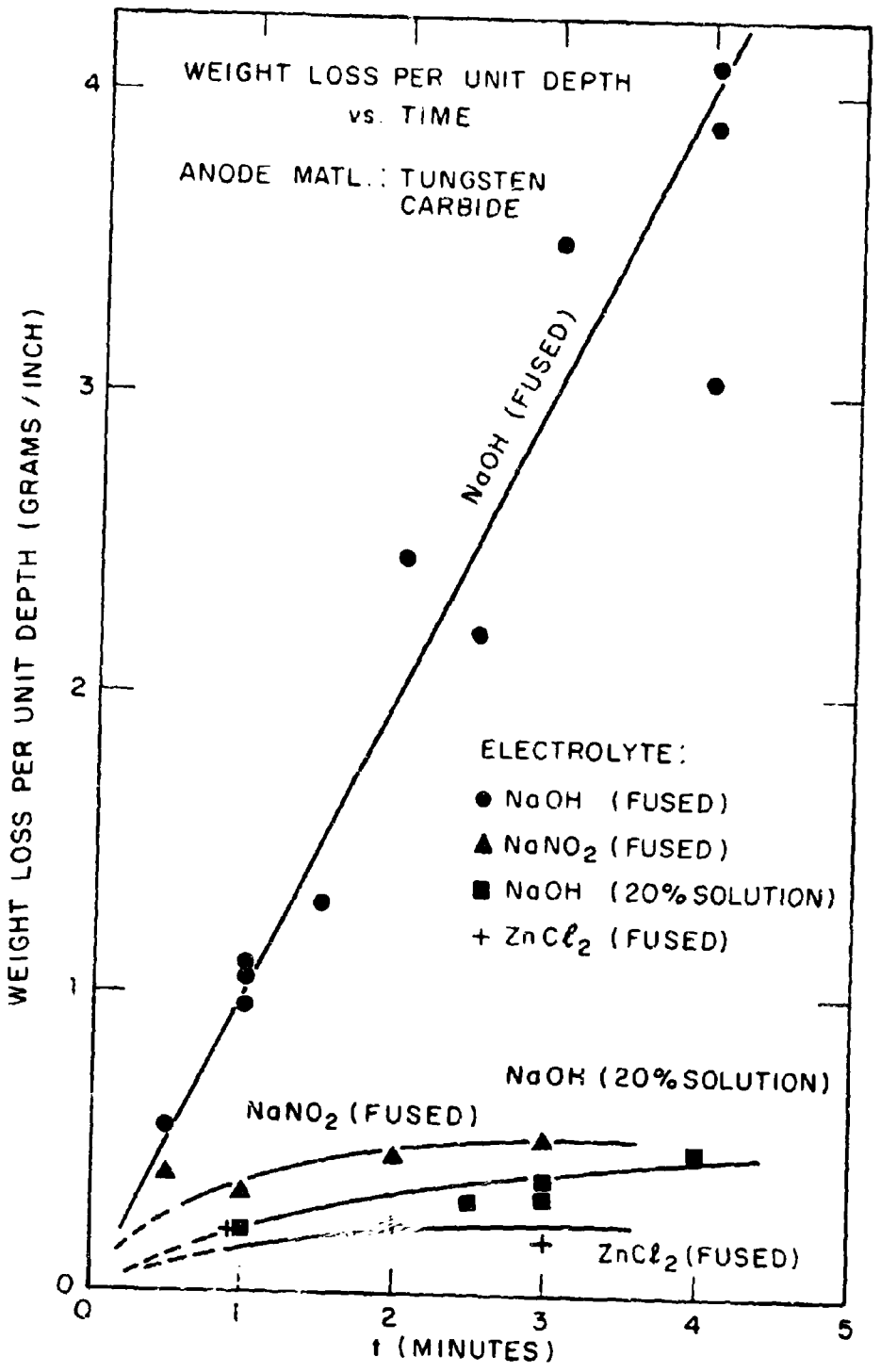
WEIGHT LOSS PER UNIT DEPTH
vs. TIME
ANODE MATL.: TUNGSTEN CARBIDE
WEIGHT LOSS PER UNIT DEPTH (GRAMS / INCH)
t (MINUTES)
NaOH (FUSED)
ELECTROLYTE:
NaOH (FUSED)
NaNO2 (FUSED)
NaOH (20% SOLUTION)
+ ZnCl2 (FUSED)
NaOH (20% SOLUTION)
NaNO2 (FUSED)
ZnCl2 (FUSED)
0
1
2
3
4
5

Fig. 4-2

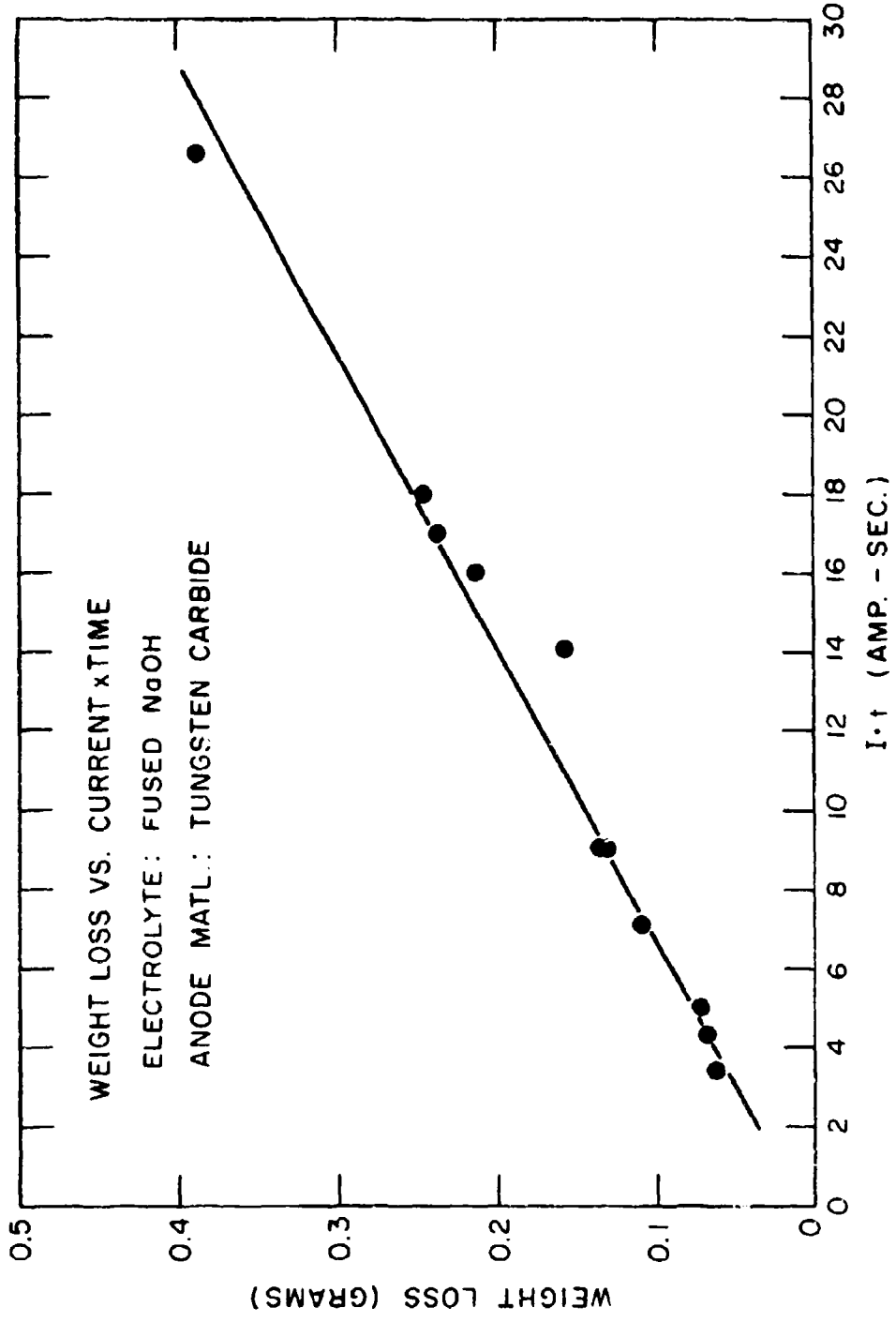
WEIGHT LOSS VS. CURRENT x TIME
ELECTROLYTE: FUSED NaOH
ANODE MATL.: TUNGSTEN CARBIDE
WEIGHT LOSS (GRAMS)
0.5
0.4
0.3
0.2
0.1
0
0
2
4
6
8
10
12
14
16
18
20
22
24
26
28
30
I·t (AMP. - SEC.)

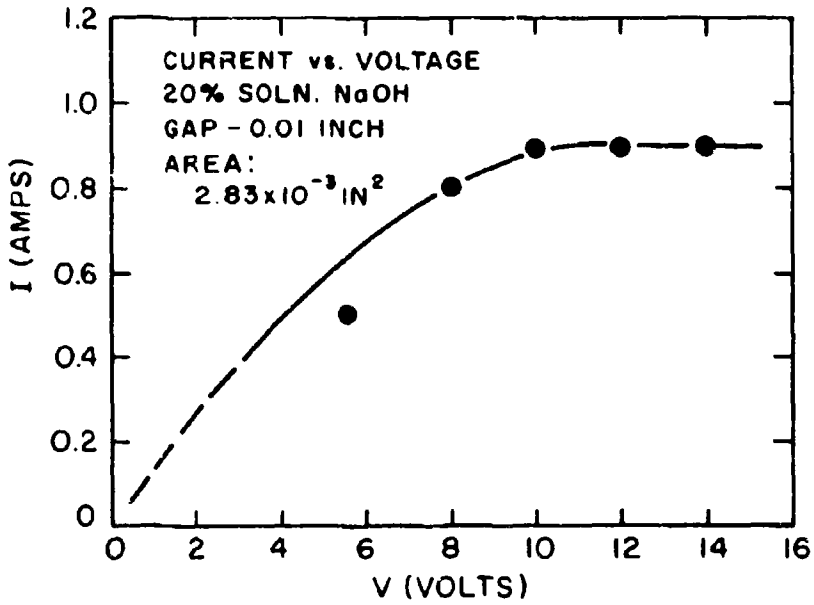

Fig. 4-4

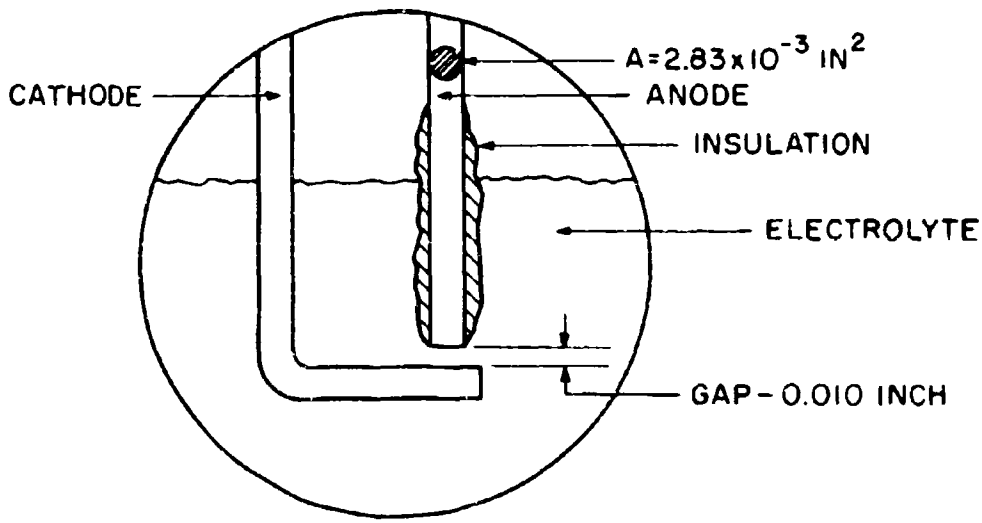

Fig. 4-5 MAXIMUM CURRENT DENSITY APPARATUS

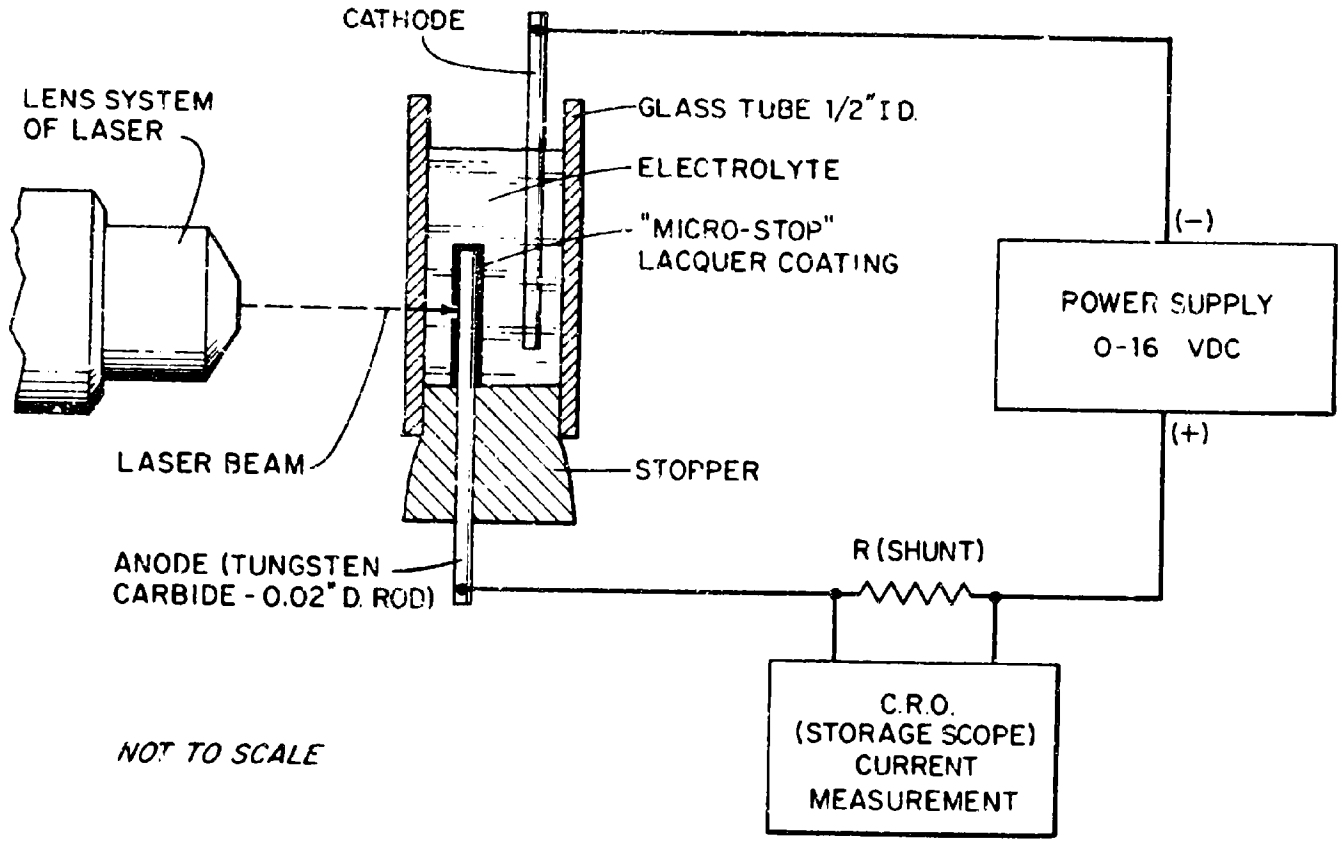

Fig. 5-1 LASER AND E.C.M. CELL

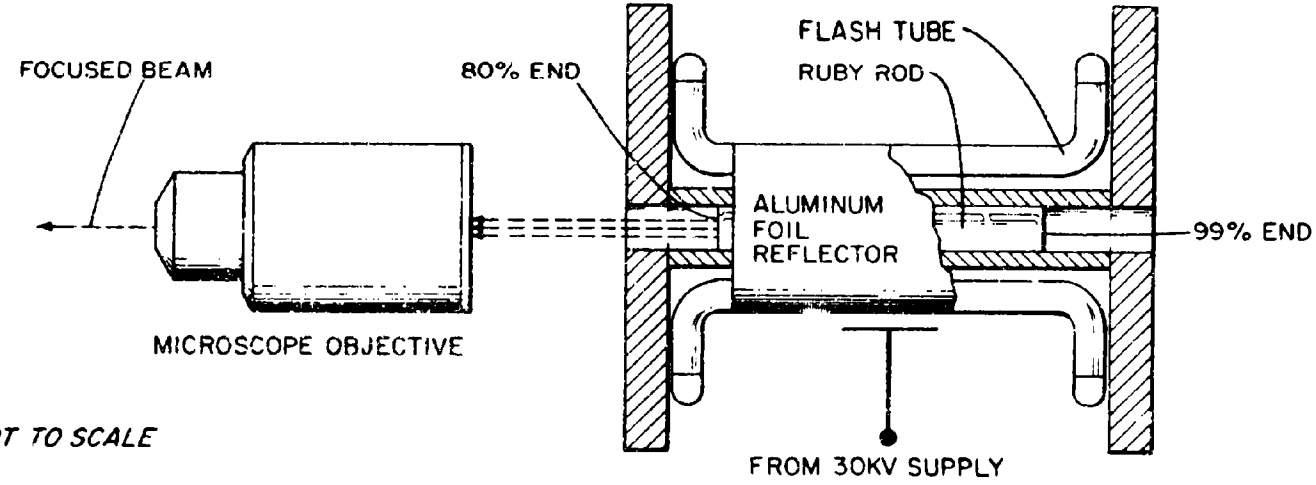

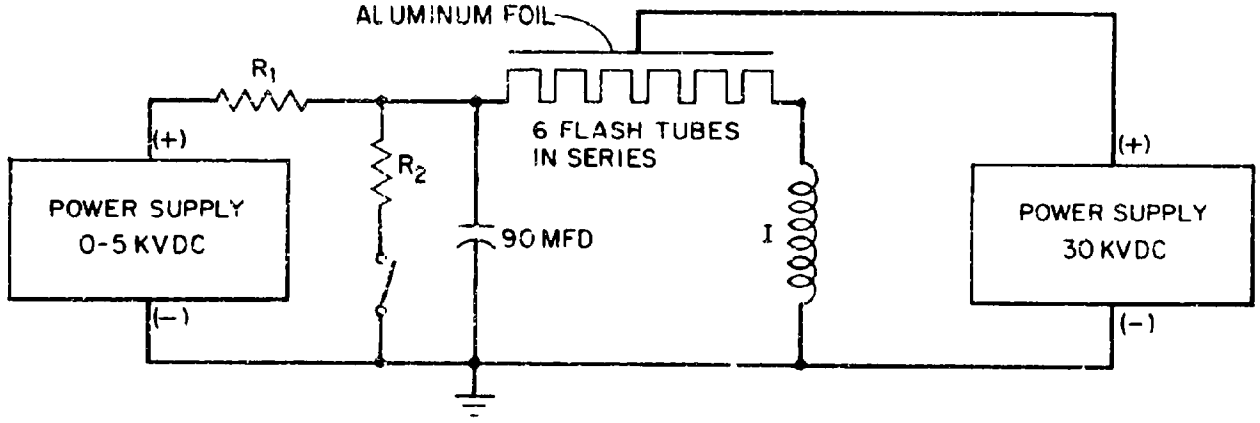

Fig. A3-1 LASER AND CIRCUIT DIAGRAM

VII. PHOTOGRAPHS AND DETAILED DRAWINGS

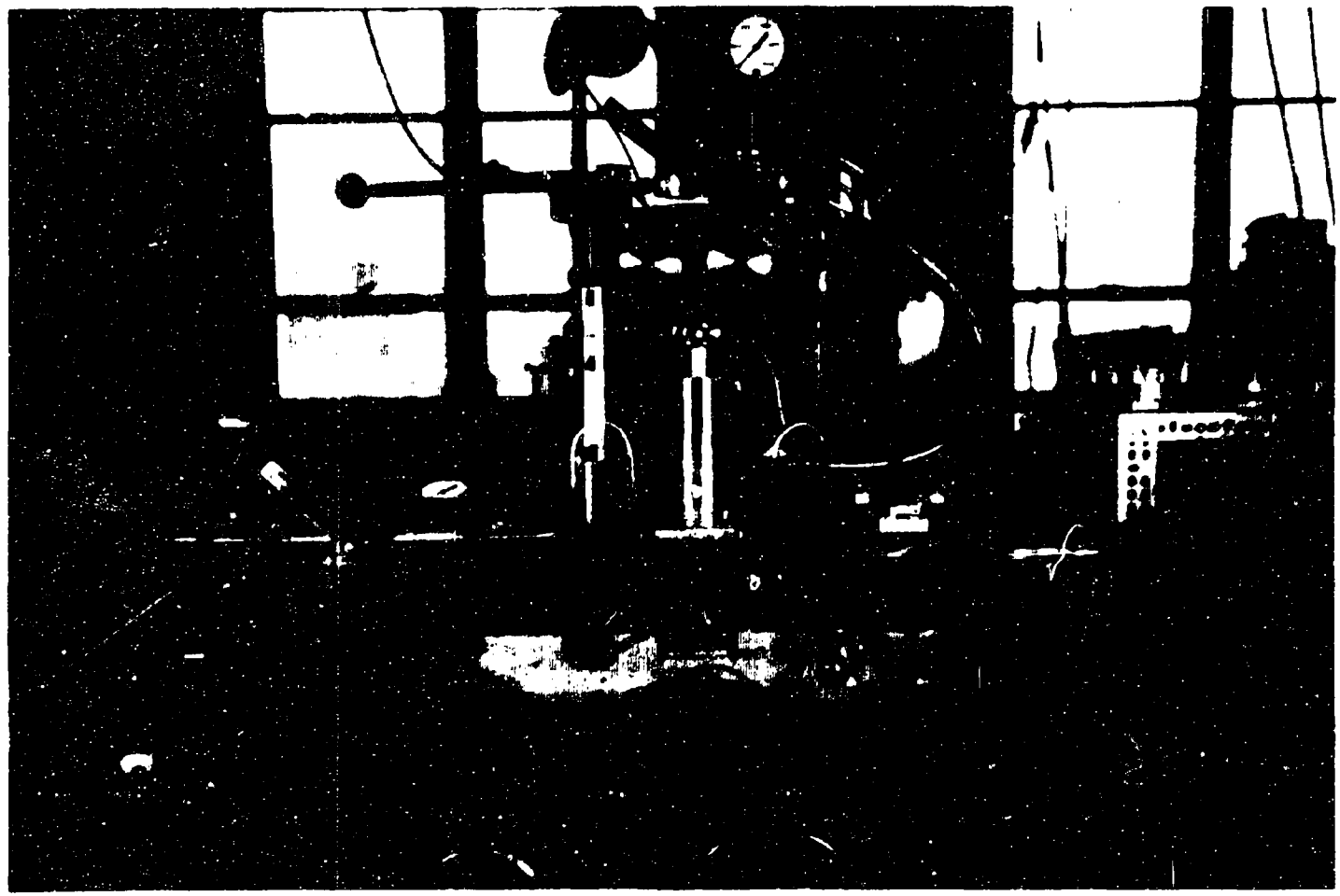

Fig. A7-1 Overall Milling Machine Setup

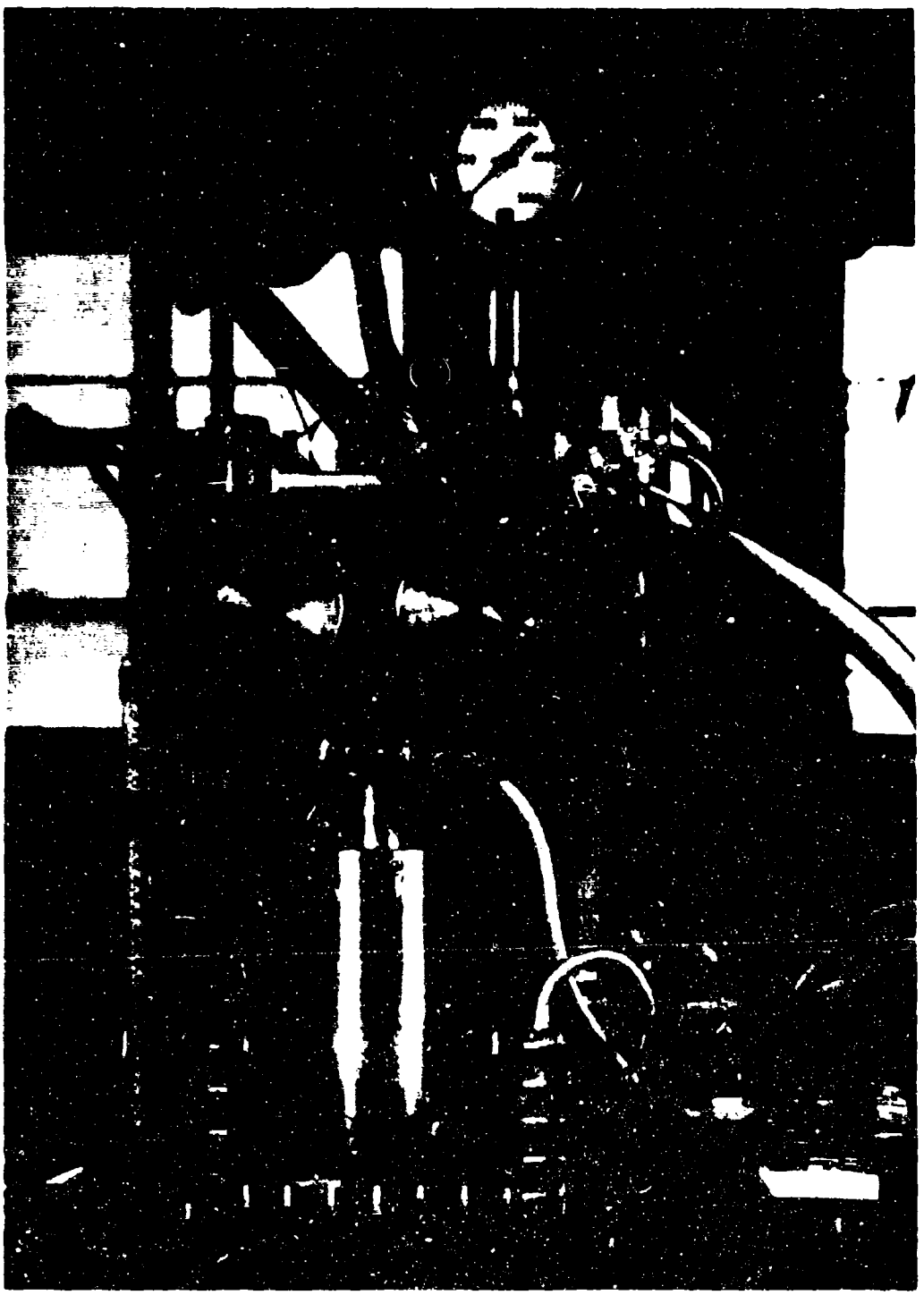

Fig. A7-2 Pressure Chamber Mounted on Milling Machine Ready for Testing Top; Tool Throttling Valve and Tool Pressure Gauge

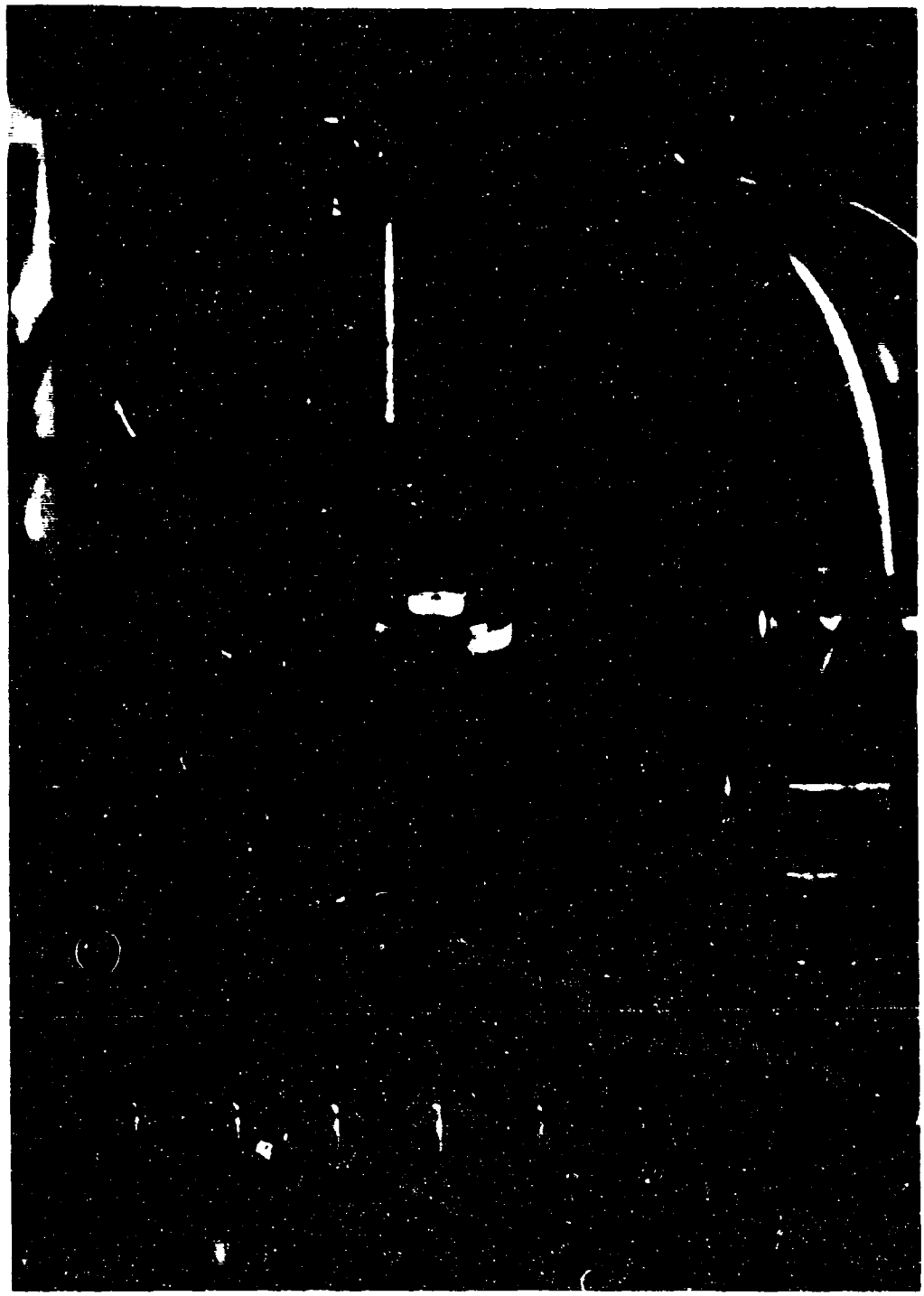

Fig. A7-3 Workpiece Mounted on Contact Electrode, Head Removed

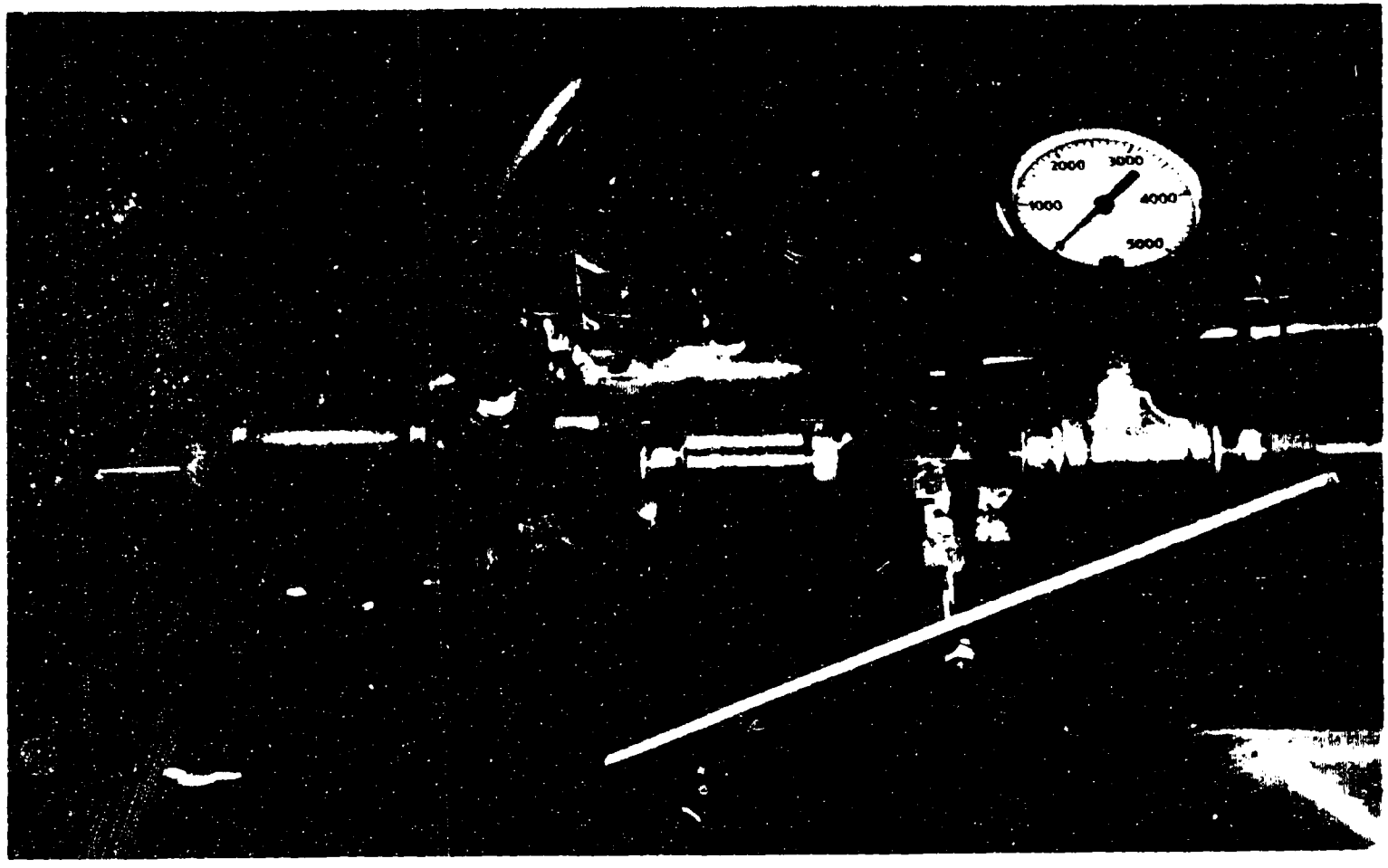

Fig. A7-4 Equipment for Regulating Pressure and Flow in Pressure Chamber
Left; Pressure Regulator Middle; Throttling Valve Right; Chamber Pressure Gauge

Fig. A7-5 Electrolyte Feed System

Fig. A7-6 Auxiliary Motor for Driving Vertical Feed

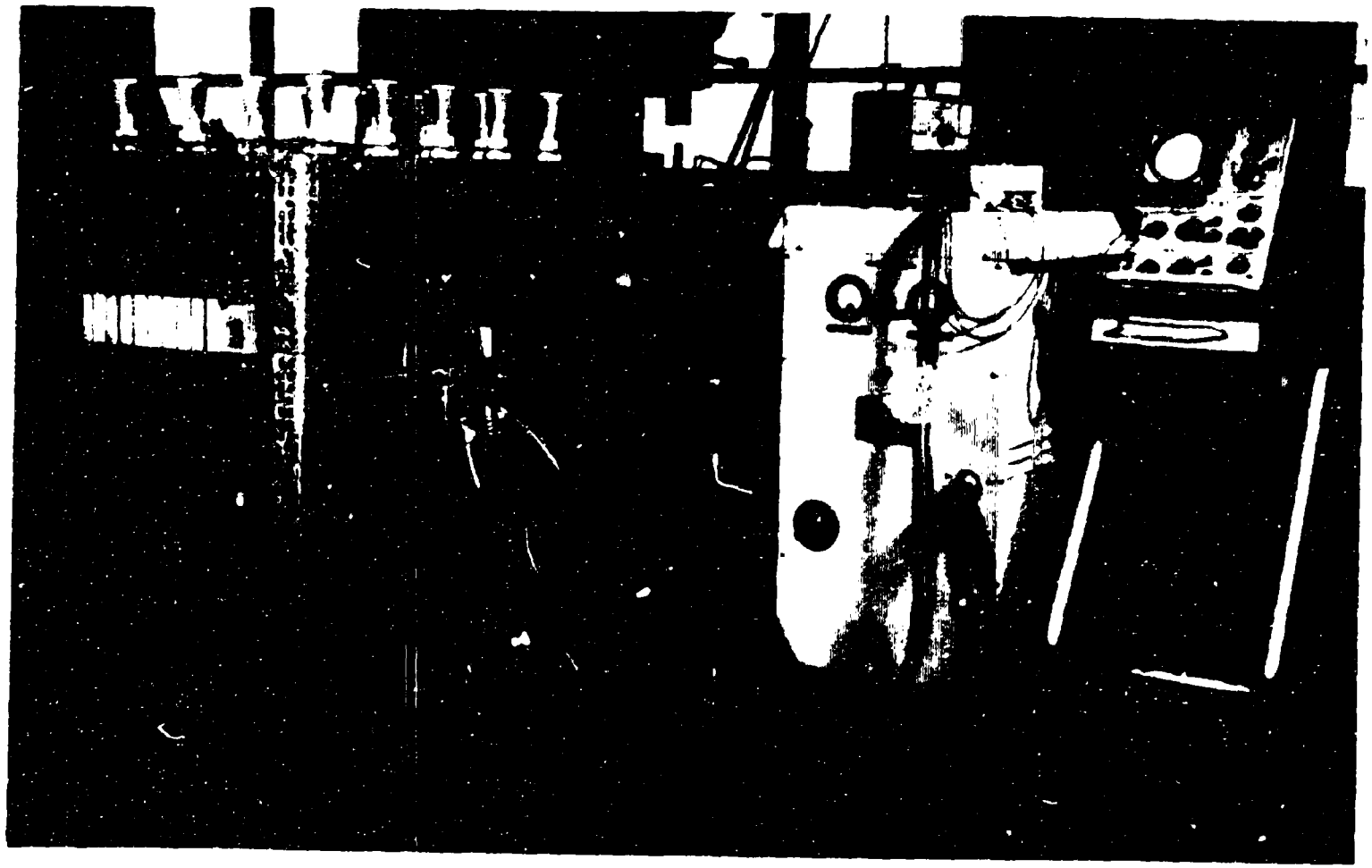

Fig. A7-7 Left; Switching System for Supplying Pulsed E.C.M. Current
Middle; Two D.C. Rectifiers Used to Supply E.C.M. Current

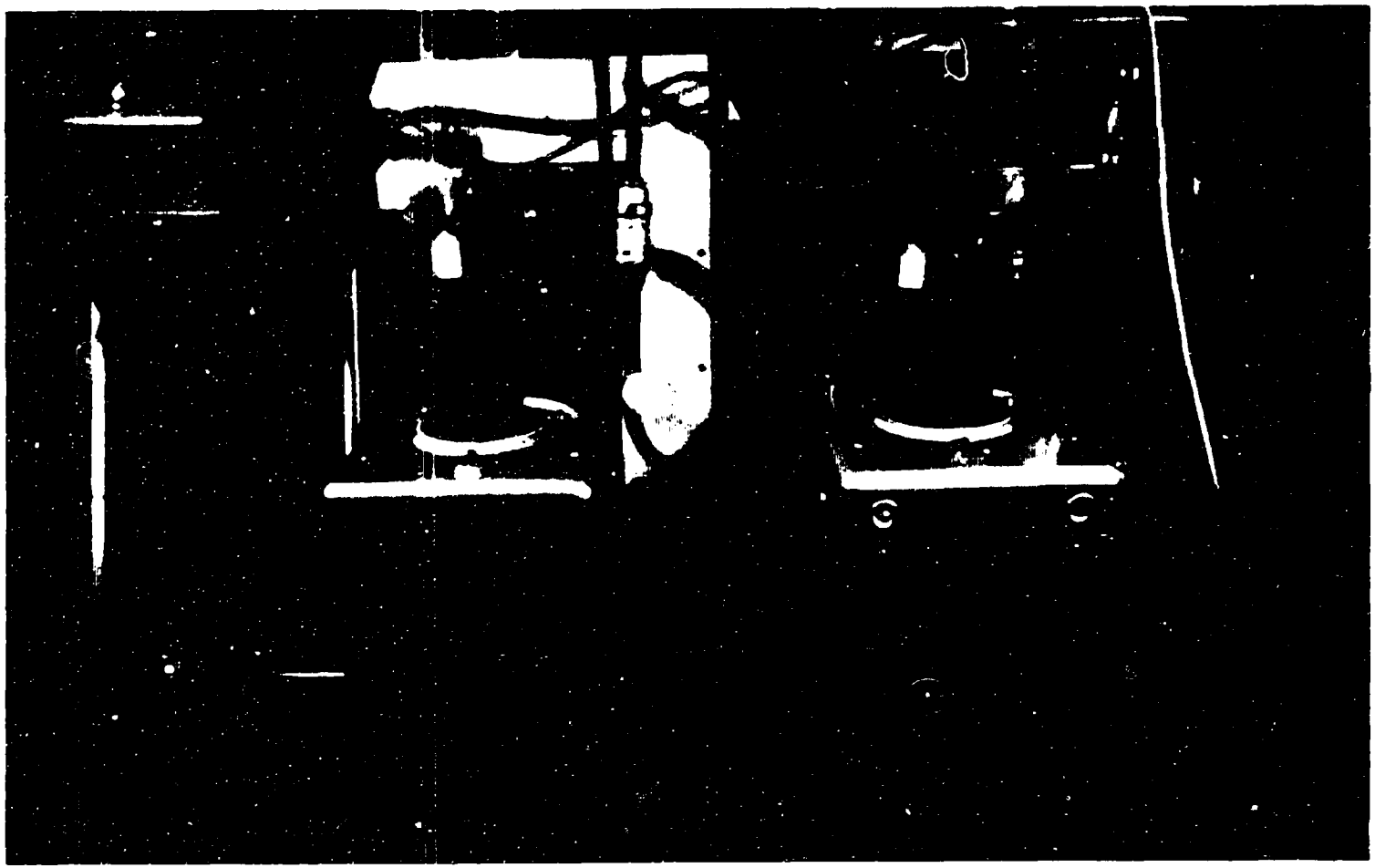

Fig. A7-8 Background; Two D.C. Rectifiers Used to Supply E C.M. Current
Foreground; Two Variacs Used to Control Voltage

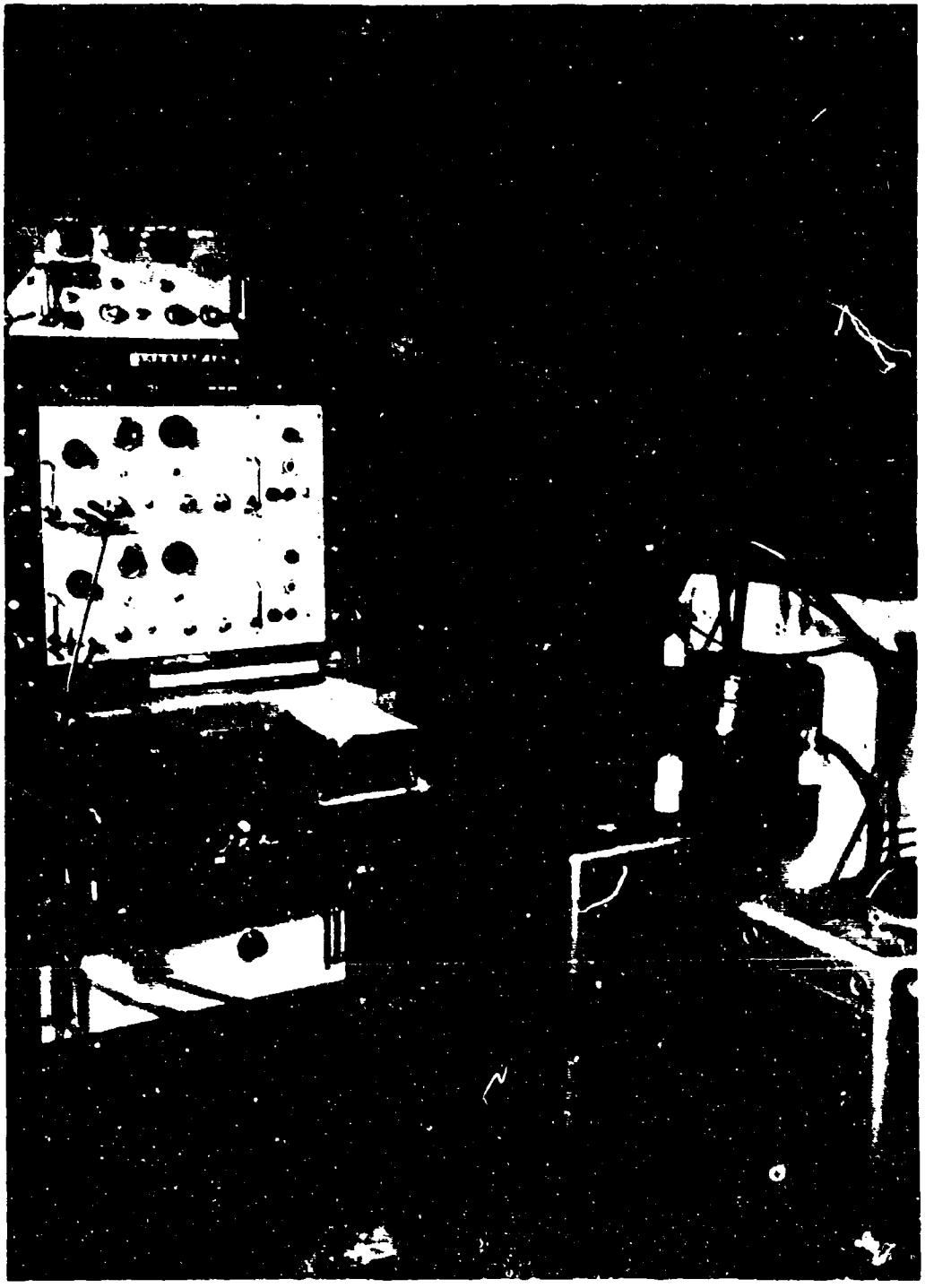

Fig. A7-9 Electrical Recording Equipment

Fig. A7-10 Four Specimens Mounted in Bakelite, Tested in Pressure and Sectioned. Showing Tool Used to Drill Each Hole

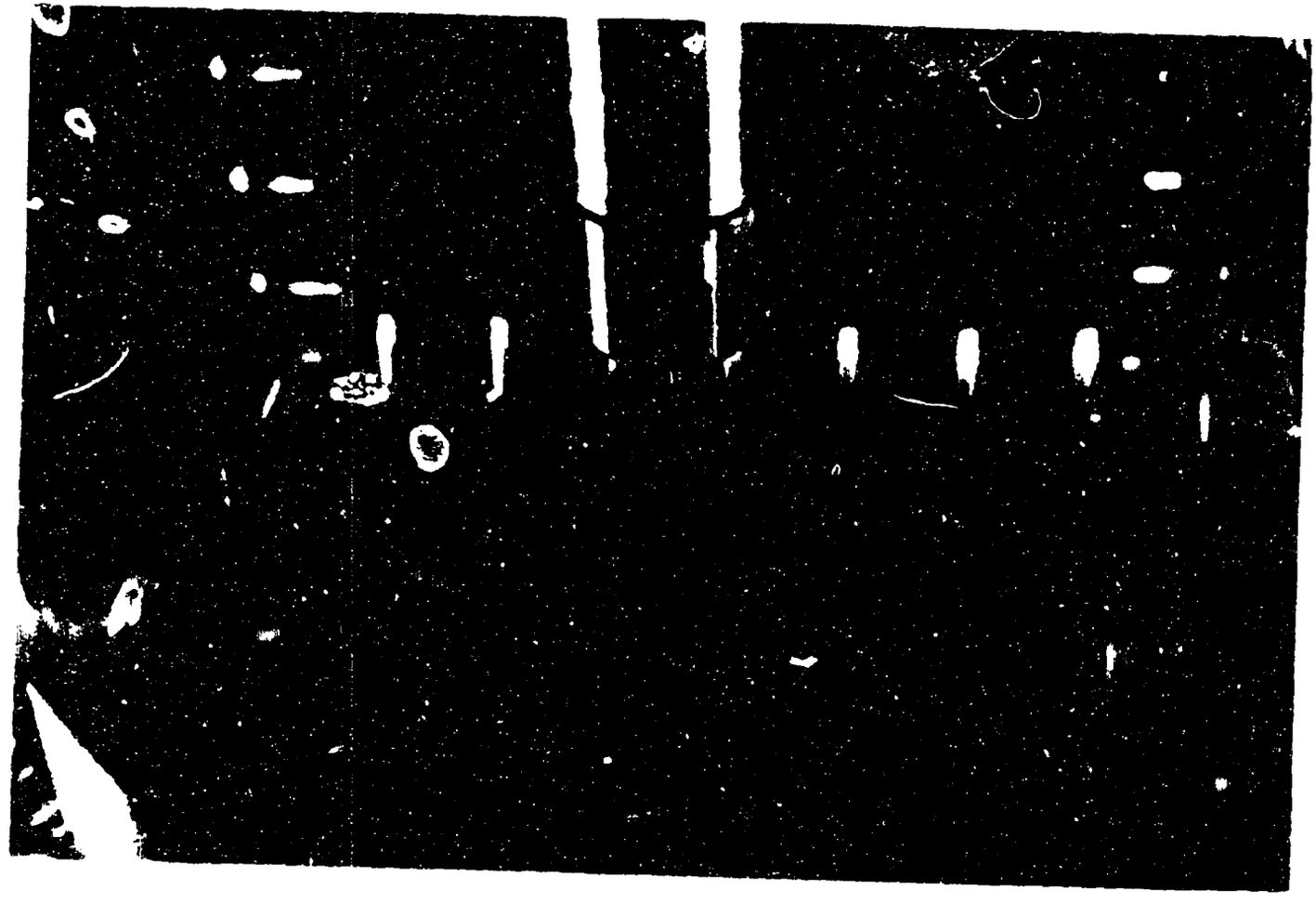

Fig. A7-11 Specimen in Flexiglas Tank. Hold Down Clamps not Shown

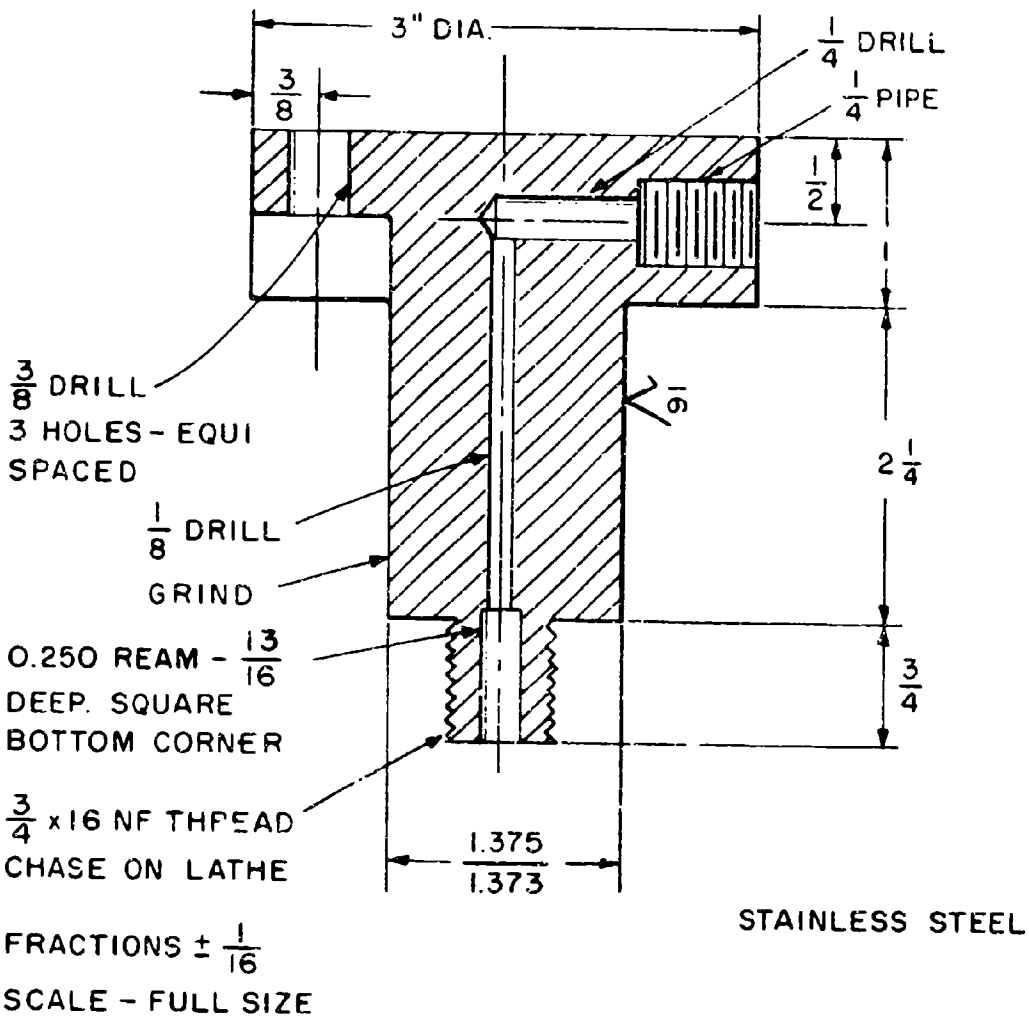

Fig. ELECTRO - CHEMICAL TOOL HOLDER

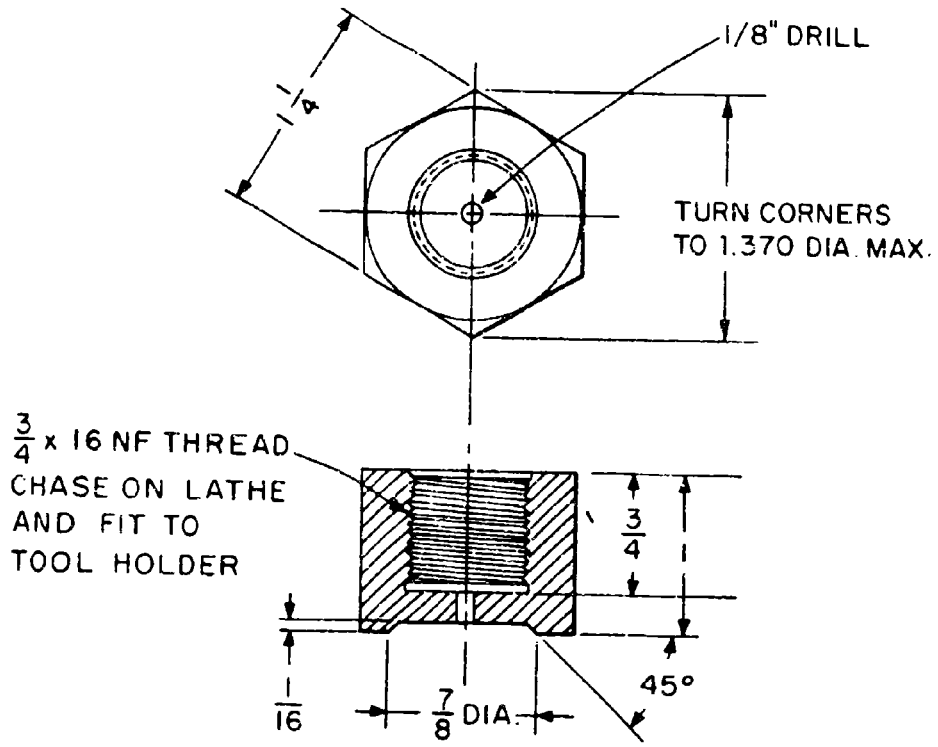

FRACTIONS ± 1/64

STAINLESS STEEL

SCALE - FULL SIZE

Fig. A7-13 TOOL LOCK-NUT

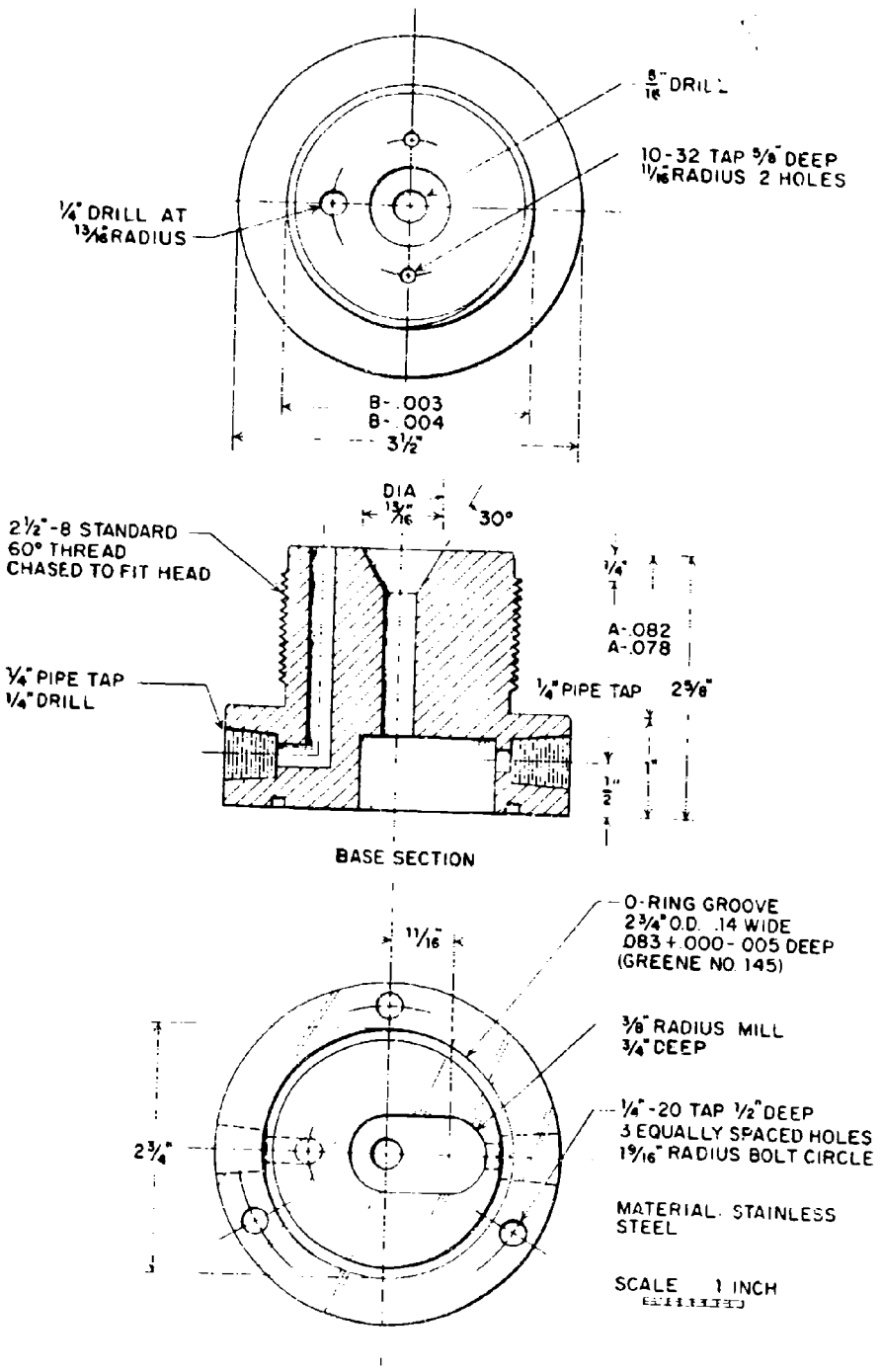
10-32 TAP 5/8" DEEP
11/16" RADIUS 2 HOLES
1/4" DRILL AT
13/16" RADIUS
B-.003
B-.004
3 1/2"
DIA
13/16"
30°
2 1/2"-8 STANDARD
60° THREAD
CHASED TO FIT HEAD
1/4" PIPE TAP
1/4" DRILL
1/4" PIPE TAP
A-.082
A-.078
2 5/8"
1"
1/2"
BASE SECTION
11/16"
O-RING GROOVE
2 3/4" O.D. .14 WIDE
.083 + .000 - .005 DEEP
(GREENE NO. 145)
3/8" RADIUS MILL
3/4" DEEP
1/4"-20 TAP 1/2" DEEP
3 EQUALLY SPACED HOLES
1 9/16" RADIUS BOLT CIRCLE
2 3/4"
MATERIAL: STAINLESS
STEEL
SCALE 1 INCH

Fig. A7-14

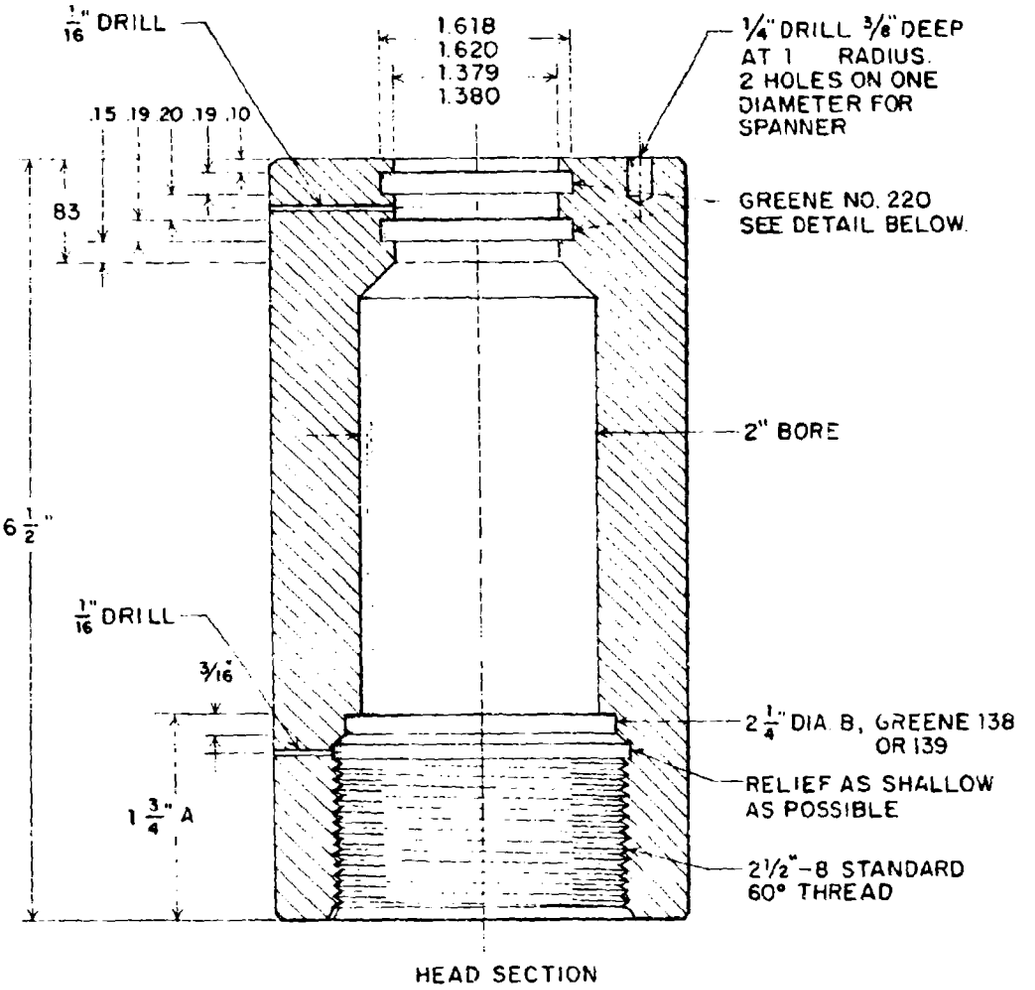

HEAD SECTION

SCALE: 1 INCH MATERIAL: STAINLESS STEEL

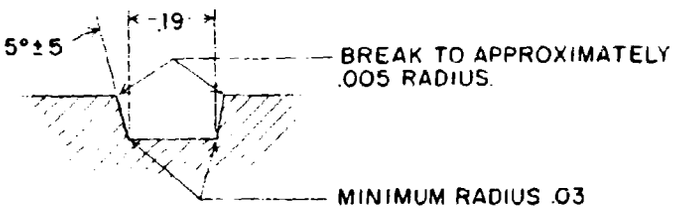

DETAIL OF GROOVE SHAPE

Fig. A7-15

BIBLIOGRAPHY

1. Chartier, Daniel J., "Electrode Materials in Electrochemical Machining", S.M. Thesis, Mech. Eng. Dept., M.I.T., August, 1964.

2. Cleary, J. F. (Ed.), G. E. Transistor Manual, General Electric Company, 1964.

3. Cole, Reno R., and Hopenfeld, Yoram, "An Investigation of Electrolytic Jet Polishing at High Current Densities". ASME Paper 60-WA-71, 1962.

4. Cook, Nathan H., Manufacturing Analysis, Addison-Wesley Publishing Co., Inc., Reading, Massachusetts, 1966.

5. Cunningham, Frederick Eliot, "The Use of Lasers for the Production of Surface Alloys", S.M. Thesis, Mech. Eng. Dept., M.I.T., June, 1964.

6. Faust, Charles L, "Electrochemical Machining of Metals", Transactions of the Institute of Metal Finishing, Vol. 41, 1964.

7. Final Report on Electrotylic Machining Development, Technical Documentary Report No. ML-TDR-64-313, Sept. 1964.

8. Foertmeyer, E. Evens., "The Versatile Metal Removal Process" ASME Technical Paper 643, 1964.

9. Gutzwiller, F. W. (Ed.) G. E. Silicon Controlled Rectifer Manual, General Electric Company, 1964.

10. Hopenfeld, J. and Cole, R.R., "Electrochemical Machining - Prediction and Correlation of Process Variables", ASME Paper 66-Prod-5, 1966.

11. Pitschke, F.A., "Electrolytes for ECM Process". ASME Technical Paper 706, 1965.

12. Pogeler, Allen, "The Electrochemical Machining of Copper in Fused Salts", 2.866 Lab. Report, Dept of Mech. Eng., M.I.T, March, 1966.

13. Williams, Lynn A. "Electrolytic Machining for Ordinary Metals", ASTME Technical Paper 642, 1964.

14. Zimmerman, Joel, "Feasibility Studies of New Electrochemical Machining Methods" S.M. Thesis, Dept. of Navel Architecture, M.I.T., June, 1964.

Security Classification

DOCUMENT CONTROL DATA - R&D

(Security classification of title, body of abstract and indexing annotation must be entered when the overall report is classified)

1 ORIGINATING ACTIVITY (Corporate author) U.S. Army Materials Research Agency Watertown, Massachusetts 02172	2a REPORT SECURITY CLASSIFICATION Unclassified 2b GROUP

3 REPORT TITLE

Increasing Electrochemical Machining Rates

4 DESCRIPTIVE NOTES (Type of report and inclusive dates)

5 AUTHOR(S) (Last name, first name, initial)

Cook, Nathan H.
Loutrel, Stephen P.
Meslink, Michael C.

6 REPORT DATE	7a TOTAL NO OF PAGES	7b NO OF REFS
January 1967	118	14

8a CONTRACT OR GRANT NO	9a ORIGINATOR'S REPORT NUMBER(S)
DA-19-066-AMC-268(W) b PROJECT NO DA Project-6261 Pema 6261 c AMCMS Code-4930.1.6261.00.01 d	AMRA GR67-03(F) CR67-03(F) 9b OTHER REPORT NO(S) (Any other numbers that may be assigned this report)

10 AVAILABILITY/LIMITATION NOTICES

Distribution of this Document is Unlimited

11 SUPPLEMENTARY NOTES	12 SPONSORING MILITARY ACTIVITY
	Watertown Arsenal

13 ABSTRACT

Phenomena which may limit the rate of Electro-Chemical-Machining (ECM) are postulated, and indirectly studied by attempting their elimination. Of the mechanisms studied, three appear most promising:

1. Elevated electrolyte pressure in the ECM zone reduces boiling, cavitation, and formation of hydrogen bubbles. As a result, drilling rates of 1.5 in/min have been attained at current densities up to 19,700 amps/in^2. This can be compared with a typical "maximum" rate of 1/4 in/min.

2. The use of fused salt electrolytes (such as NaOH) appears quite promising for difficult-to-ECM materials such as tungsten-carbide.

3. Pulsed DC current with short reverse spikes appears promising for materials such as tungsten-carbide which normally form relatively impervious reaction layers.

DD FORM 1 JAN 64 1473

Unclassified
Security Classification

KEY WORDS	LINK A		LINK B		LINK C	
	ROLE	WT	ROLE	WT	ROLE	WT
Electro Chemical Milling						
Drilling						
Metal Removal						
Alloy Steels						
Tungsten Carbide						
Nickel Allcys						
Cobalt Alloys						

INSTRUCTIONS

1. ORIGINATING ACTIVITY: Enter the name and address of the contractor, subcontractor, grantee, Department of Defense activity or other organization *(corporate author)* issuing the report.

2a. REPORT SECURITY CLASSIFICATION: Enter the overall security classification of the report. Indicate whether "Restricted Data" is included. Marking is to be in accordance with appropriate security regulations.

2b. GROUP: Automatic downgrading is specified in DoD Directive 5200.10 and Armed Forces Industrial Manual. Enter the group number. Also, when applicable, show that optional markings have been used for Group 3 and Group 4 as authorized.

3. REPORT TITLE: Enter the complete report title in all capital letters. Titles in all cases should be unclassified. If a meaningful title cannot be selected without classification, show title classification in all capitals in parenthesis immediately following the title.

4. DESCRIPTIVE NOTES: If appropriate, enter the type of report, e.g., interim, progress, summary, annual, or final. Give the inclusive dates when a specific reporting period is covered.

5. AUTHOR(S): Enter the name(s) of author(s) as shown on or in the report. Enter last name, first name, middle initial. If military, show rank and branch of service. The name of the principal author is an absolute minimum requirement.

6. REPORT DATE: Enter the date of the report as day, month, year; or month, year. If more than one date appears on the report, use date of publication.

7a. TOTAL NUMBER OF PAGES: The total page count should follow normal pagination procedures, i.e., enter the number of pages containing information.

7b. NUMBER OF REFERENCES: Enter the total number of references cited in the report.

8a. CONTRACT OR GRANT NUMBER: If appropriate, enter the applicable number of the contract or grant under which the report was written.

8b, 8c, & 8d. PROJECT NUMBER: Enter the appropriate military department identification, such as project number, subproject number, system numbers, task number, etc.

9a. ORIGINATOR'S REPORT NUMBER(S): Enter the official report number by which the document will be identified and controlled by the originating activity. This number must be unique to this report.

9b. OTHER REPORT NUMBER(S): If the report has been assigned any other report numbers *(either by the originator or by the sponsor)*, also enter this number(s).

10. AVAILABILITY/LIMITATION NOTICES: Enter any limitations on further dissemination of the report, other than those imposed by security classification, using standard statements such as:

(1) "Qualified requesters may obtain copies of this report from DDC."

(2) "Foreign announcement and dissemination of this report by DDC is not authorized."

(3) "U. S. Government agencies may obtain copies of this report directly from DDC. Other qualified DDC users shall request through _____."

(4) "U. S. military agencies may obtain copies of this report directly from DDC. Other qualified users shall request through _____."

(5) "All distribution of this report is controlled. Qualified DDC users shall request through _____."

If the report has been furnished to the Office of Technical Services, Department of Commerce, for sale to the public, indicate this fact and enter the price, if known.

11. SUPPLEMENTARY NOTES: Use for additional explanatory notes.

12. SPONSORING MILITARY ACTIVITY: Enter the name of the departmental project office or laboratory sponsoring *(paying for)* the research and development. Include address.

13. ABSTRACT: Enter an abstract giving a brief and factual summary of the document indicative of the report, even though it may also appear elsewhere in the body of the technical report. If additional space is required, a continuation sheet shall be attached.

It is highly desirable that the abstract of classified reports be unclassified. Each paragraph of the abstract shall end with an indication of the military security classification of the information in the paragraph, represented as *(TS)*, *(S)*, *(C)*, or *(U)*.

There is no limitation on the length of the abstract. However, the suggested length is from 150 to 225 words.

14. KEY WORDS: Key words are technically meaningful terms or short phrases that characterize a report and may be used as index entries for cataloging the report. Key words must be selected so that no security classification is required. Identifiers, such as equipment model designation, trade name, military project code name, geographic location, may be used as key words but will be followed by an indication of technical context. The assignment of links, rules, and weights is optional.